Master's thesis

NTNU
Norwegian University of Science and Technology
Faculty of Natural Sciences
Department of Materials Science and Engineering

Tor-Eivind Ebbesen

Addition of Secondary Aluminium in SandCast Aluminium-Silicon Alloys

Master's thesis in Materials Science and Engineering
Supervisor: Ola Jensrud
July 2020

NTNU
Norwegian University of
Science and Technology

Tor-Eivind Ebbesen

Addition of Secondary Aluminium in SandCast Aluminium-Silicon Alloys

Master's thesis in Materials Science and Engineering
Supervisor: Ola Jensrud
July 2020

Norwegian University of Science and Technology
Faculty of Natural Sciences
Department of Materials Science and Engineering

NTNU
Norwegian University of
Science and Technology

Preface

This report is a master thesis written for the department of material science and technology at NTNU. In this project work the use of recycled aluminium in sand cast componentes is investigated. The project work was carried out during the spring semester of 2020, with close cooperation with SINTEF Industry as a part of the ALUMAR project.

Acknowledgements

The author would first of all like to thank Ola Jensrud and Morten Onsøien for great help and guidance throughout this project work. I would also thank Arne Nordmark and Kurt Sandaunet for the practical help in the casting of my samples.

A much appreciative thanks should also go to Stanka Tomovic Petrovic for the completion of the SEM results. In addition I would like to thank Pål Christian Skaret and Marit Olaisen for the tensile testing. A thank you will also go out to Berit Vinje Kramer for the guidance and training in the material testing labs.

Abstract

For this master thesis the aim was to investigate the effect the additon of alloying elements like copper, iron, zinc, nickel and manganese has on an AlSi10Mg alloy and find an optimal heat-treatment program for said alloys. These alloying elements was added to 5 different alloys with an increasing amount. This addition was added to represent the addition of recycled aluminium.

Various test was conducted on the casted alloys, first a heat-treatment was found. Then some mechanical testes like tensile testing and hardness measurements was completed. Before the samples was investigated by optical microscope and scanning electron microscope.

It was found that the optimal heat-treatment program was the T6 program, with solution heat-treatment at 535°C for 8h, water quenching and artificial aging at 175°C for 8h. The mechanical properties and the grain size for the alloys was effected by the various amounts of alloying elements.

From the results gathered throughout this project, it is reasonable to conclude that the use of recycled aluminium in the casting process is a good idea as long as it is not added in to large amounts. With the environmental and economical advantages gained from use of recycled aluminium, the use of recycled aluminium would be recommended for this casting process.

Sammendrag

For denne masteroppgaven var målet å undersøke effekten tilsetningen av legeringselementer som kobber, jern, sink, nikkel og mangan har på en AlSi10Mg-legering. Samt å finne et gunstig varmebehandlingsprogram for nevnte legeringer. Disse legeringselementene ble tilsatt til 5 forskjellige legeringer med en økende mengde, disse skulle representere tilsetningen av resirkulert aluminium.

Forskjellige tester ble utført på de støpte legeringene, først ble det funnet en gunstig varmebehandling. Deretter ble noen mekaniske tester som strekkprøving og hardhetsmålinger gjennomført. Prøvene ble til slutt undersøkt med optisk mikroskop og skanningselektronmikroskop.

Det ble funnet at det gunstigste varmebehandlingsprogrammet var T6-programmet, med innherding ved 535°C i 8 timer, vannkjøling og utherding ved 175°C i 8 timer. De mekaniske egenskapene og kornstørrelsen for legeringene blir påvirket av den forskjellige mengden legeringselementer.

Fra resultatene samlet gjennom dette prosjektet er det rimelig å konkludere med at bruk av resirkulert aluminium i støpeprosessen er en god idé, så lenge det ikke tilføres for store mengder. Med de miljømessige og økonomiske fordelene som oppnås ved bruk av resirkulert aluminium, vil bruk av resirkulert aluminium anbefales for denne støpeprosessen.

Contents

List of Figures

List of Tables

Chapter 1

Introduction

Aluminium is one of the most widely used metals on earth and it is still developing to wider use. Its excellent properties makes it a desired metal for many different applications, like aerospace, car industry, offshore applications, food packaging and much more. Pure aluminium on its own is relatively weak, but its low density 2.7g/cm^3 makes it a desirable on its own. When the pure aluminium is mixed together with different alloying elements, its true powers emerges. By alloying the aluminium with the right element you can achieve many of your desired properties. With an increase in knowledge about the different aluminium alloys and its alloying elements, the use of aluminium in future applications will grow. With advanced knowledge about this the aluminium can replace iron amongst other, in many applications. Aluminium is also 100% recyclable which makes it very relevant when you want to spare the environment[1].

The offshore industry is one of the industries that has started to appreciate all the good attributes aluminium have, its low weight and corrosion resistance to name a few makes it a desired metal. One of these companies is NORSE metal, who delivers large sand casted aluminium parts to the offshore industry. Perfecting this sand casting process, and the final product will put NORSE metal forward as a highly sought after supplier for aluminium parts to the offshore industry. They have therefore hired SINTEF to investigate and research how to improve this casting process. Finding a new aluminium alloy with the right alloying elements, use of more recycled aluminium, heat-treatment and so on is what has to be researched in order to improve the casting process.

The goal for the ALUMAR project at SINTEF is to improve the whole casting process for the AlSiMg alloy that NORSE metal is sand casting. By finding the right alloying elements, investigating the use of recycled aluminium and finding a optimal heat treating program.

This master thesis is meant to contribute to reaching the goals of the ALUMAR project and by doing so helping NORSE metal in optimising their casting process. This will be done by investigating the use of recycled aluminium in various amounts, testing optimal heat-treatment program and conducting various material tests on the casted products. This master thesis is a continuation on the work done by Ebbe-

sen in the fall of 2019[2]. In this work 5 different aluminium alloys was sand casted into different shapes that were investigated. There were meant to cast new alloys for this master thesis, but due to the extraordinary situation that has effected the world, this had to be put on hold for someone else to do, when there is time for that. Other experiments like a corrosion test was planned, but had to be cancelled.

So as the continuation of the work done last semester is shortened down. The main goal for this master thesis is to do a heat-treatment on the plates that was casted, and investigate the effect this has on the different alloys and the effect of using more recycled aluminium. By doing tensile testing, hardness testing, optical microscope, scanning electron microscope (SEM) and electrical conductivity. The results will then give a good discussion basis for how to improve the casting process at NORSE metal. Since this is a continuation of work done by the author last semester, some of the results gathered there will be discussed in this thesis along with some of the same theoretical background.

1.1 Previous work

This master thesis is a continuation of work done by Ebbesen[2]. In this work 5 different aluminium alloys containing an increasing amount of recycled aluminium was sand casted into different shapes that were design to test the fluidity and castabillity of the alloys. The increasing amount of recycled aluminium was represented by adding alloying elements like Fe, Mn, Zn, Cu and Ni with an increasing amount from the first alloy L1 to the last alloy L5. Here it was found by a feeding test that the porosity of each alloys was effected by the alloying elements. Where the L1 had the highest amount of porosity. The porosity decreased from L1 to L3, before increasing a small amount from L3 to L5[2].

A tensile test was also conducted on the alloys, finding that the yield strength and the ultimate tensile strength (UTS) increased with an increased amount of alloying elements. While the ductility seemed to remain somewhat the same, except for L5 where the ductility dropped. Finally the grain structure was investigated with an optical microscope, here it was found that the grain size seem to increase with the addition of the alloying elements[2].

Chapter 2

Theoretical Background

In this chapter the theoretical background for the master thesis is presented. An introduction to aluminium and its alloys, casting process, heat-treatment and some material testing methods will be presented.

2.1 Aluminium and aluminium alloys

The state of art and related work were reviewed, and an identification of the relevant background material were carried out in the project preceding this thesis[2]. No relevant new material was found during the work on the thesis. The presentation from the project report is included below.

Aluminium and its alloys is mostly known for its low density ($2.7g/cm^2$), good corrosion resistance in some environments and high thermal and electrical conductivity. The low density makes this material highly applicable for uses where a low weight is wanted. Most of the aluminium alloys are easy to form due to a high ductility. The FCC crystal structure of the aluminium keeps the high ductility even at low temperatures, making it easy to form at low temperatures. Aluminium has a relatively low strength in its pure form, but this can be improved by cold work or by alloying. These processes does however tend to decrease the general corrosion resistance of the metal[1].

The most commonly used alloying elements for aluminium include magnesium, silicon, manganese, zinc and copper. The addition of these different alloying elements will give different classifications of the aluminium alloys[1].

2.1.1 Alloying elements

The state of art and related work were reviewed, and an identification of the relevant background material were carried out in the project preceding this thesis[2]. No relevant new material was found during the work on the thesis. The presentation from the project report is included below.

The main alloying elements in this project is silicon, copper, magnesium, manganese, zinc and nickel. They have different effects on the aluminium when added.

Copper is mostly used as the main alloying element in the 2xxx casting alloys. The copper is added to mainly increase the strength in the alloy and forms one of the strongest aluminium alloys[3]. An increased amount of copper is known for decreasing the ductility and the corrosion resistance of a aluminium-silicon alloy alloys[4, 5]. The copper is therefor only present at a maximum of 0.05 or 0.1%[3]. However a study done by VDS showed that copper addition $< 0.4\%$, had little effect when looking at the atmospheric corrosion. But when exposed to a liquid environment the results was less impressive[6].

Silicon is one of the most important alloying elements in aluminium casting alloys. Use of silicon in a aluminium alloy improves the castabillity of aluminium alloys due to better fluidity and lower shrinkage of molten aluminium-silicon alloys. It has a low density of 2.34 g/cm^3 which helps in keeping a low weight in the cast component[7]. An increase in the use of silicon will increase the strength of the alloy as well as it improves the resistance to abrasive wear. Silicon in combination with magnesium allows to strengthen the alloys by precipitation hardening heat-treatment[5, 8].

Magnesium hardens and strengthen the alloys without considerable decrease in ductility, this is done by solution hardening mechanisms. Magnesium in combination with silicon allows to strengthen the alloys by precipitation hardening heat-treatment, where Mg_2Si precipitates is formed[5, 8]. It can give a good corrosion resistance and high strength[7].

Manganese is used to change the iron-bearing phases type in secondary casting alloys, by changing the iron phases from β needles to α-script, this results in an improvement in the ductility and feeding[3]. The addition of manganese will improve low cycle fatigue resistance and the ductility of aluminium alloys containing silicon and iron. It also increases the corrosion resistance, making it more applicable for marine components[5, 8]. If the content of manganese in an aluminium alloy precedes 0,5 wt.% it has been found that the ultimate tensile strength (UTS) and the yield strength increases significantly, without a decrease in ductility[7].

Zinc strengthens the alloys by precipitation hardening heat-treatment, if it's in combination with magnesium or magnesium-copper. It also increases susceptibility to stress corrosion cracking[5, 8]. Zinc is usually only present in 7xxx-series of aluminium alloys and in secondary aluminium, it is neutral in a way that it does not change an alloy's properties by itself[5, 8].

Nickel increases hardness and strength of aluminium-copper and aluminium-nickel at higher temperatures. It also reduces the thermal expansion coefficient, making it more applicable for higher temperature applications[5, 8].

Iron is the most common impurity found in aluminium, but its sometimes added to some alloys to improve the strength. When iron is added the ductility decreases[5, 8]. In Al-Si alloys the amount of iron should be kept as low as possible, in order to avoid reduction in the fracture toughness and ductility. To high levels of iron could also cause a decrease in casting productivity due to shrinkage porosity[7]. A high

iron volume fraction may also affect the fluidity and feeding in a negative way[3].

2.1.2 Al-Si-Mg alloy

Aluminium-Silicon alloys is one of the most used alloys in the casting industry, due to their excellent fluidity and castabillity. A good corrosion resistance also makes it applicable for a maritime environment[3]. These attributes can be further improved by modification of the aluminium-silicon eutectic. This modification is especially relevant for sand casting, where strontium is added as the modification mechanism[3]. The addition of magnesium to the Al-Si alloys forms a basis for alloys with a great casting abilities, that can also improve their properties by heat-treatment after the casting[3].

In a study done by Hailin Yang And Co[9]. The Effect of nickel on an Al-Mg-Si-Mn alloy was investigated. The results in this study showed that the presence of Ni in the alloy encourage the formation of Ni-rich intermetallics. These intermetallics has a dendritic morphology during primary solidification and lamellar morphology during the eutectic solidification stage. The formation of Ni seemed to always appear in relation with iron. As for the mechanical effects of nickel the yield strength increased slightly, while the elongation decreased significantly. The UTS had a slight increase with addition of small amounts of Ni (>0.16%), but the UTS dropped in value when a larger amount of nickel was added[9].

In another study done by Xiaofeng Wang and Co[10]. The Effect of Zn on the microstructure, texture and mechanical properties of an Al-Mg-Si-Cu alloy was investigated, with a medium number of Fe-rich phase particles. The authors found that the addition of Zn had a significant influence on the mechanical properties, where it increased the yield strength, UTS and elongation. The results also showed that Zn is beneficial to reduce particles[10].

In a study done by Magnus Sætersdal Remøe the effect of various alloying elements on the ductility of Al-Mg-Si alloys was investigated[11]. He conducted various experiments on four different alloys with different concentrations of Si, Mg, Fe, Cu and Mn. With a tensile test he found that the addition of Copper gave an increase in strength, without decreasing the ductility significantly. The element that had the most positive effect on the ductility was the addition of Manganese. These two alloying elements added together gave the best combined properties, when it comes to ductility and strength[11]

2.1.3 Secondary aluminium

The recycling of aluminium started less then 20 years after the commercialisation of the Hall-Heroult process in 1888[12]. Aluminium has many attributes that makes it suitable for recycling, the low energy required to remelt the aluminium compared to the production of primary aluminium and its good corrosion resistance. Today secondary aluminium produced from scrap is nearly half of the produced aluminium in Europe and North America, with an further growth predicted[12]. The production of secondary aluminium form scrap has several of advantages. First of all it

reduces up to 90% of the energy cost required to produce the metal and by that reducing the overall environmental impact of the aluminium production. It also offers a cheaper way to produce alloys, instead of adding alloying elements to primary metal[12]. One of the biggest differences from primary to secondary aluminium is the concentration of hydrogen. The concentration is larger in the secondary aluminium, mainly due to the use of fossil fuel to melt the scrap used in the recycling process[12].

As mentioned the production of secondary aluminium is started form aluminium scrap from various sectors. This aluminium scrap consists of various aluminium alloys, with various alloying elements. When the secondary is produced from this scrap these different alloys is mixed together, giving a product that contains these various alloying elements[13]

2.2 Heat-treatment

Heat treating a metal is a process where the metal is heated and cooled under controlled conditions in order to improve the performance, durability and properties of the metal[14]. It is possible to control the microstructure by heat treating the metal, making it easier to process. The heat-treatment can as mentioned improve the durability by making it more corrosion resistant, wear resistant or more fatigue resistant. All metals can be heat treated, aluminium alloys are often annealed or solutionized, quenched and age hardened[14].

2.2.1 Heat-treatment of aluminium alloys

The strength of casted aluminium alloys is possible to improve and to control with heat-treatment. It is possible to control the size, shape and distribution of the impurity elements in the casting[15]. There are different temper designations for the different aluminium alloys, this is due to the different properties required for their applications[15]. These designations has been standardised by the Aluminium Association[16]:

- F: As-fabricated.
- O: Annealed.
- T4: Solution heat treated and naturally aged.
- T5: Artificially aged from F temper.
- T6: Solution heat treated, quenched and artificially aged.
- T7: Solution heat treated, quenched and overaged.

The solution treatment, quenching, preaging and artificial ageing is 4 different steps that is used in the heat-treatment process. These steps is all important, but as the listing over shows it is not necessary to employ all of them. Each step have different effect on each alloy, it is therefor important to have a good understanding in what each step does.

2.2.2 Precipitation hardening and solution heat-treatment

There are two basic requirements for strengthening an alloy by precipitation hardening. The first one is that the process must result in an very fine precipitate dispersed in the matrix. And the other one is there must be a degree of lattice matching between the precipitate particles and the matrix. Meaning that for a effective precipitation hardening it is necessary that a coherent or a semi-coherent interface is present[17]. When a lattice distortion is produced by a coherent precipitate the impending dislocation motion results in a strengthening. A miss-match in size between the solute atoms and the solvent is caused because the fully coherent clusters of solute phase are groupings with the same crystal structure as the solvent phase. This results in quite a lot of strain, this cluster then stabilizes dislocations since dislocations often reduce strain. This eventually results in a strengthening and hardening of the alloy[17].

One of the necessities to precipitation hardening is the ability to heat the alloy to temperature where all the solute is dissolved and a single phase structure is achieved[17]. This is then the basis for solution heat-treatment. When the alloy in question is heated up to a temperature above the solvus temperature and held at this temperature for a sufficient amount of time a single phase is then formed, which is the solution heat-treatment. This structure is then retained at lower temperatures by cooling the alloy rapidly by water quenching for instance[17]. Precipitation is then achieved after the quenching by heating the alloy to a temperature below the solvus temperature and holding it there for a certain time. As the alloy is held at this temperature the precipitates nucleates at the grain boundaries for instance. The region in the matrix surrounding the precipitates is reduced in solute content, since the precipitates has a higher solute content than the matrix[17].

2.2.3 Quenching

Quenching is the rapid cooling of a metal from the solution temperature mentioned in chapter 2.2.2. The main objective for the quenching is to maintain the metastable solid solution that is formed in the solution heat-treatment[18]. With the quenching is sufficiently rapid solute atoms can form zones of homogeneous precipitation for strengthening by age hardening at RT(Room Temperature). The quenching is also used to keep the number of vacant lattice sites to a minimum, in order to help with low-temperature diffusion during the aging stage of precipitation hardening[18].

2.2.4 Heat-treatment of casted Al-Si-Mg alloys

Casted Al-Si-Mg alloys are used in a large variety of application, due to its excellent castability, good fatigue properties and corrosion resistance. The strength and ductility of the alloy can also be improved to a desired combination, by heat-treatment. The heat-treatment results in a formation of Mg_2Si precipitates during ageing that gives the increase in tensile properties, these properties variate by the duration of the solution and the ageing process and the temperature used[17].

2.3 Casting of aluminium

2.3.1 Casting of aluminium alloys

Casting of aluminium has played an integral part in the growth of the aluminium industry. Aluminium is amongst very few metals that can be shape cast by many different casting processes like the sand casting, pressure die casting, plaster mould and more. Where the pressure die casting is the most dominant method contributing to 70% of the aluminium, shape castings. The aluminium cast alloys is versatile and have many favourable characteristics. good fluidity, low melting point, chemical stability and good as-cast surface finish is some of abilities that makes these alloys desirable[19].

Sand mould casting

The state of art and related work were reviewed, and an identification of the relevant background material were carried out in the project preceding this thesis[2]. No relevant new material was found during the work on the thesis. The presentation from the project report is included below.

The general principal for casting is pouring a metal in its liquid state into a mould with a shape of your choosing and let it solidify into its solid state. The solid state will then be the same as the mould. There are three main reasons for using casting. It's used when the desired shape is complicated or large, when a alloy has a low ductility that makes it not suitable for forming by hot/cold working or it will be used based on a economical stance[1].

Sand casting has the same principal, the material is melted in a furnace before it is poured into the mould, which is made out of sand. The sand mould has been formed to the desired shape, so when the liquid metal is poured into the casket it will solidify as the desired shape. When the metal begins to cool and solidify, you can try to control the solidification rate to avoid rapid cooling that may result in cracks, shrinkage or incomplete sections. After the solidification is completed the sand mould is broken so that the casting can be taken out. Since the sand mould is broken it can not be used again, makes this process less economical

The use of casting as a production route will welcome some problems. One of the problems that can occur is the local variation of the microstructure, causing compositional variations. This defect can lead to variations in results of different properties. The ultimate tensile strength and elongation, will variate due to the difference in microstructure. Finer microstructure does normally give better mechanical properties due to the smaller differences in microstructure[20]. Sand casted metals usually have a rough surface that can have impurities and surface vibrations[21].

In the transport sector the use of casting dominates in the production of engine blocks, pistons, wheels and so on. Sand casting is most commonly used for thick walled products or for parts that need an hollow interior[21]. The casting of aluminium alloys has improved in many ways over the years, but porosity still poses

issues for the casting engineer. But also here there has been developed some techniques for minimizing the porosity. By improving the design and melt handling, degassing and filtration the industry has managed to minimize the porosity in aluminium casting. However it is still a topic that has room for improvement. The porosity will weaken the cast, by reducing the mechanical properties, it will worsen the machinability and give a overall appearance on the cast that is not wanted[21]. One of the main reasons for porosity in casted aluminium alloys is the appearance of hydrogen gas in the molten aluminium. Because hydrogen is the only gas that has significant solubility in aluminium[21]. When the molten aluminium solidifies, this hydrogen can create porosity because of its low solubility in the solid. The measures that can be made to prevent this is to degas the molten metal by adding tablets that can remove the hydrogen or react with it. Or just bubbling inert gas through the molten metal[21].

Microstructure

The mechanical properties of the casted aluminium alloys is highly dependent on the microstructure. This microstructure can variate depending on what alloying elements is used and the composition. The grain size is one of the main variables that control the mechanical properties, by using grain refinement the grain size can be controlled. The addition of TiB during the casting process will reduce the grain size, giving a finer grain structure[5][8]. The grain size can also be controlled by vibration, control of metal flow and stirring during the casting process[22].

The biggest effect on the microstructure on a casted aluminium alloy is the effect of eutectic mixture that surrounds the aluminium crystal, especially in Al-Si alloys. In these alloys the primary silicon may form before the eutectic[21]

Modification

For aluminium cast alloys that contains large amount of eutectic, like the aluminium-silicon alloys. The eutectic morphology and the dendrite arm spacing determine the properties more than the grain size[22]. Therefore in sand casting of aluminium-silicon alloys, the use of eutectic modification like strontium is used to change eutectic silicon into fibrous elements. In sand casting of Al-Si alloys it is also common to use eutectic modification, to change the eutectic silicon from coarse platelike into fine fibrous elements[22].

The modification of an Al-Si alloy is complex subject with conflicting theories. An alloy that is not modified will have a poor ductility due to the large flakes of brittle silicon[23]. Applying a modification treatment will cause the silicon to assume a fine, fibrous structure. This treatment will then result in an improved elongation. The modification result of modification with strontium is represented in figure 2.1. Initially sodium was the first used modifier, but due to its low solubility in molten aluminium and rapid loss to oxidation it has been replaced by strontium. which is added via master alloys with nearly 100% recovery together with a slow loss to oxidation[23]. The addition of the strontium increases the tensile strength, elongation at break and improves the ductility and machinability[5][8].

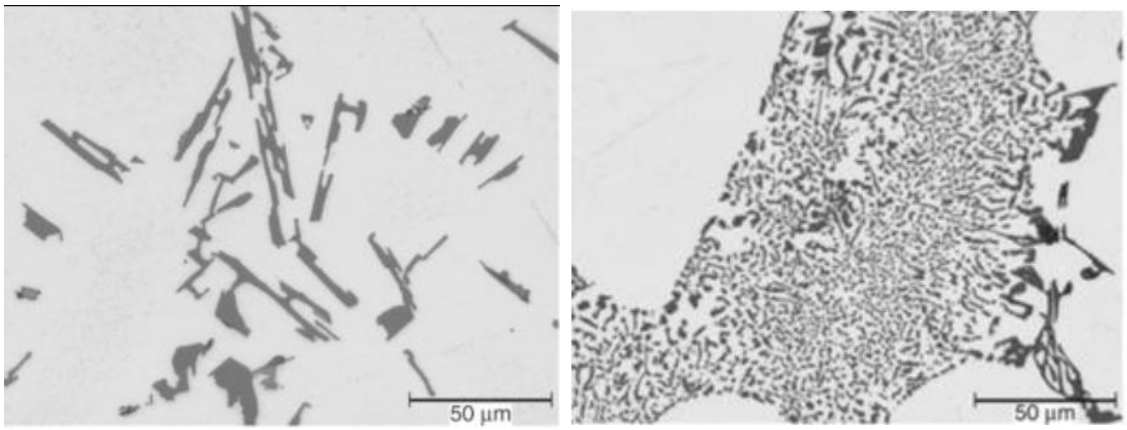

(a) (b)

Figure 2.1: Microstructure of A356 alloy before strontium modification (a) and after strontium modification (b)[23]

2.4 Material quality testing

2.4.1 Tensile testing

The state of art and related work were reviewed, and an identification of the relevant background material were carried out in the project preceding this thesis[2]. No relevant new material was found during the work on the thesis. The presentation from the project report is included below.

Tension tests is one of the most frequently used mechanical stress-strain tests. The test specimen is applied a load uniaxially along the longest part. When loaded the specimen will start to deform and with increasing load it will eventually fracture. The material is normally machined so the cross section of the middle part is reduced compared to the edges[1]. This is to assure that the possibility of fracture at the edges is reduced. When placed in the machine its tightened at the ends, it will then elongate the specimen at a constant rate. During this it will gather the data of the applied load as well as the successive elongation[1].

When the machine has collected the data for the elongation and the force, the data can be used to calculate the engineering strain (ϵ) and stress (σ), the young's moudulus (E) as well as the tensile and yield strength. The engineering stress and strain can be caluclated from equation 2.1 and 2.2, where A is the area of the cross-section before the test was initiated and F is the applied force[1].

$$\sigma = \frac{F}{A_0} \tag{2.1}$$

$$\epsilon = \frac{\Delta l}{l_0} \tag{2.2}$$

Plotting these will give a stress-strain curve that will give the values for the the young's modulus, yield and tensile strength, ultimate tensile strength and fracture

strength as shown in figure 2.2. The young's modulus is given by Hooke's law, shown in equation 2.3[1].

$$\sigma = E\epsilon \tag{2.3}$$

The ductility can also be found from a tensile test. This is a measure of the degree of plastic deformation sustained before the material goes to fracture, this value can be expressed as the percent elongation (%EL). This value is the percentage of plastic strain at fracure and is given by equation 2.4 where l_f is the fracture length and l_0 is the original length

$$\%EL = \frac{l_f - l_0}{l_0} 100\% \tag{2.4}$$

Figure 2.2 shows how the Stress-strain curve can be used to find yield strength and UTS. The yield strength represent the end of the elastic part of the curve, after this point the material will start to deform plastic. The UTS is the highest stress that the material can withstand.

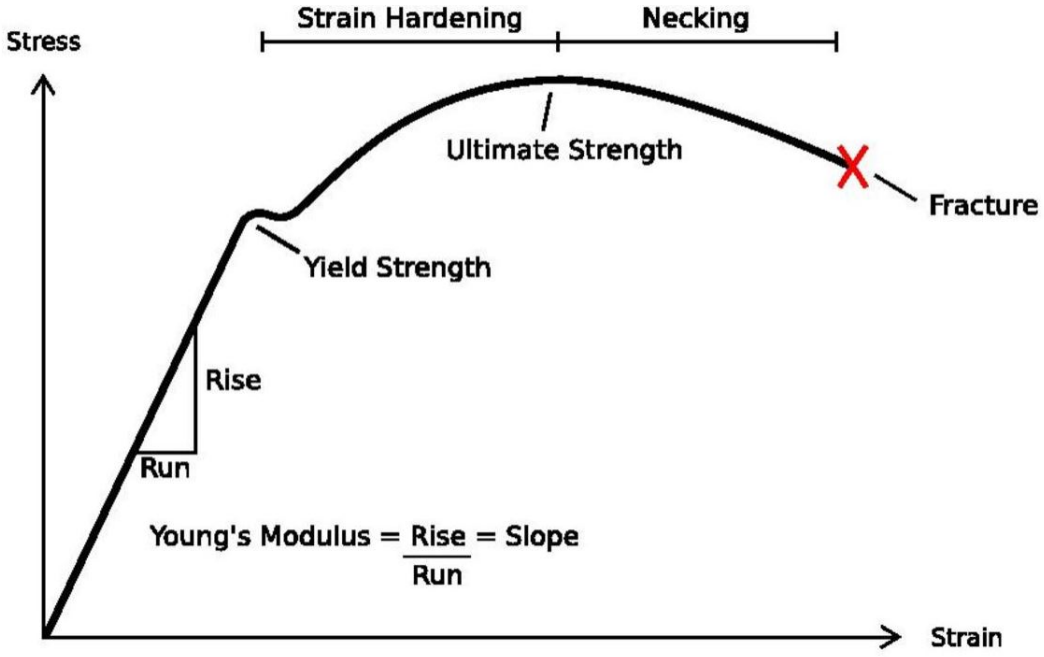

Figure 2.2: Basic stress-strain curve with indications of how to find UTS and Yield Strength[24].

2.4.2 Average grain size

When determining the average grain size the American Society for testing and Materials (ASTM) have come up with a method [25]. This method uses straight lines and counting how many grain boundaries is crossed when drawn on pictures from i.e optical microscope or SEM. The straight lines is drawn in various directions on the picture to gain a representation of the whole area. These lines is then measured and then counted how many grain boundaries they have crossed. Equation 2.5 shows

how the average grain size ($\bar{l}$) is calculated, here P is the total number of grain boundaries crossed for all the lines combined. L_T is the total length of all the lines combined and M is the magnification used[1].

$$\bar{l} = \frac{L_T}{PM} \tag{2.5}$$

2.4.3 Hardness

Hardness is defined as a materials ability to resist deformation when applied a load. It does exist a number of methods of testing the hardness of a material, but all have a general similarities in that the tests consists of pressing some kind of indenter with a known geometry into the material. One of the main differences between the various test is the shape of this indenter. Spherical, pyramidal and conical shapes are the most used ones[26]. One of these tests is the hardness Vickers test, which uses a pyramidal shape. This test method was developed as a substitute to the Brinell test which used a spherical indenter, and was not as well suited for testing of hard steels. The pyramidal shape was more applicable for harder materials.

The general principle for the Vickers test is that the pyramidal indenter is applied to the with a known force to the material for 10 to 15s. After this time the force is lifted and a squared shape can be seen in the material, the diagonals of this square is then measured and the average is used to calculate the Hardness Vickers (HV). Figure 2.3 shows an illustration of this testing method. Equation 2.6 shows the formula used to calculate the HV, here P is the force that is applied to the metal given in gf, α is the face angle of the indenter (136°) and d is the mean diagonal given in µm[27].

$$HV = \frac{2000Psin(\alpha/2)}{d^2} = \frac{1854.4P}{d^2} \tag{2.6}$$

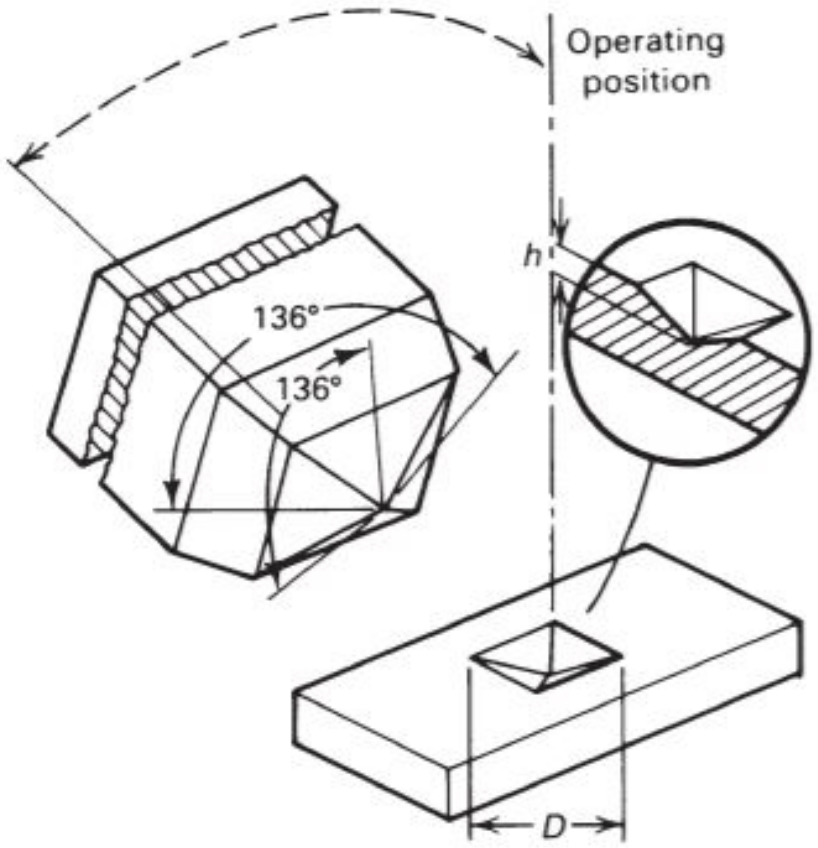

Figure 2.3: Sketch of the hardness Vickers test that shows the diamond pyramidal indenter and an example of the indent created in the material[27].

Chapter 3

Experimental Work

In this chapter the procedure in which the experimental work was completed is presented in detail. The purpose of this chapter is to give the viewer a overview of what has been done in this project and how it has been done. This chapter should be so detailed that the experiments can be repeated by anyone with the right equipment.

3.1 Procedure

With this project being a continuation of the work done in the fall of 2019 the samples are the same. These samples were delivered from hydro as a AlSi10 alloy together with different alloying elements like iron, copper, manganese, zinc and nickel. These metals will the be added to the original AlSi10 alloy through casting with increasing amounts, simulating the use of recycled aluminium.

3.1.1 Casting process

The casting of the samples used in this master thesis was done in company with SINTEF in the fall of 2019. These samples was casted as plates with dimensions 14.5cmx5.0cmx0.5cm and able to be used in various material testing and characterisation work. The casted plates was casted with 5 different batches where the amount for added alloying element increased with each step. Table 3.1 shows the desired composition of each of the 5 alloys where the the first (primary aluminium) has the lowest amount of alloying element and number 5 (secondary aluminium) has the highest amount, meaning it has the highest amount of recycled aluminium.

The first step of the casting process was weigh the required amount of metal required to achieve the desired composition for each alloy. After this was done the primary alloy was put in the induction oven seen in figure 3.1 and heated above its melting temperature. When the metal had melted the additional alloying elements was then added into the melt, then the oven was heated to a temperature well above 730°C. When this temperature was reached the casting was conducted by pouring the melted metal into a sand mould with the shape of the desired plates. The metal then solidified as the desired shape shown in figure 3.2.

Table 3.1: This table shows how much of each alloying elements is included in each step. All values are given in wt%[2].

	Si	Fe	Cu	Mn	Mg	Ni	Zn
Primary (L1)	10	0.12	0.0035	0.002	0.35	0.0047	0.0085
L2	10	0.2	0.01	0.1	0.35	0.006	0.02
L3	10	0.3	0.03	0.15	0.35	0.007	0.04
L4	10	0.4	0.05	0.20	0.35	0.008	0.06
Secondary (L5)	10	0.5	0.1	0.25	0.35	0.01	0.1

Figure 3.1: Melted aluminium in induction oven[2].

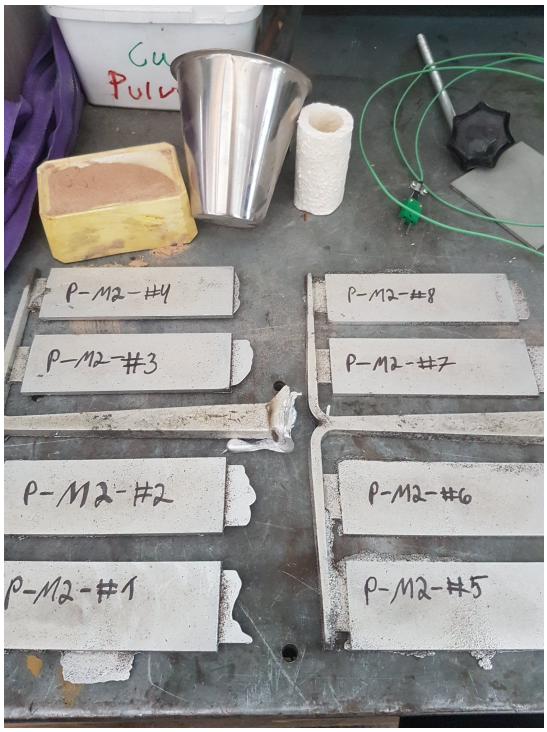

Figure 3.2: Casted Plates[2].

3.1.2 Labeling of the sample

Since the casting was already completed by Ebbesen in the work done in fall of 2019, a labeling system was already set[2]. The labeling that is relevant for this thesis is the labeling of each of the alloys. So the alloy with least amount of alloying elements is named L1 and then the next with a little more alloying elements is named L2 and so on. Until L5 which is the alloy with most alloying elements.

3.1.3 Actual composition

During the casting of the samples some of the alloying elements was added in wrong amounts resulting in a chemical composition different from the meant composition. This was found by completing a chemical composition test presented by Ebbesen in the project work[2]. Table 3.2 shoes theses results.

Table 3.2: Table of actual chemical composition for the casted alloys. All the values are given in wt%[2]

	Silicon	Magnesium	Titanium	Strontium	Iron	Copper	Nickel	Zinc
L1	9.908	0.343	0.0565	0.0223	0.122	0.0035	0.0046	0.0085
L2	9.921	0.340	0.062	0.0237	0.201	0.0104	0.00634	0.0285
L3	9.811	0.337	0.059	0.023	0.293	0.028	0.0232	0.0374
L4	9.752	0.335	0.061	0.026	0.380	0.0900	0.00833	0.0587
L5	9.884	0.333	0.0574	0.024	0.454	0.0914	0.00502	0.0997

3.2 Heat-treatment

3.2.1 Finding optimal heat-treatment program

The heat-treatment was conducted on the plates after the casting process was completed. It was necessary to find what heat-treatment program was most effective on the casted alloys, before the final heat-treatment was conducted. In order to find this program a mix of literature, simulations and testing is put together. So the literature found in the ASM handbooks show that the most commonly used program for casted AlSiMg alloys is the T6 heat-treatment program, which is described in chapter 2.2[17]. Then the temperature and time was the variating factor that had to be decided. Hydro completed a simulated heat-treatment with changes in temperature an time as variables. Giving an indication to what works best for the samples in this project.

It was then possible to go through with a physical test on the plates. The plate was cut into 24 parts in order to test out 12 different programs (2 samples for each program). All the 24 parts was solution heat treated the same way at 535°C for 8h before they where quenched in water. Then the separation started. 3 different temperatures was tested 160°C, 175°C and 190°C. Within these 3 temperatures 4 different time intervals was tested; 2h, 4h, 8h and 16h as table 3.3 illustrates.

Table 3.3: This table show the heat-treatment testing sequence, for finding the best heat-treatment program where the top row is the temperature and the bottom one is the time.

160°C				175°C				190°C			
2h	4h	8h	16h	2h	4h	8h	16h	2h	4h	8h	16h

After the heat-treatment on all the different samples was completed the testing of which program worked best began. The way the effect was test was with a hardness test. This test was done with a Innovatest manual hardness testing machine, where the hardness of each sample was tested. The hardness is measured by taking a small imprint in the material, these imprints was taken up to 10 times on each sample so that the hardness of the whole surface was tested. The average hardness of all the samples was then calculated and compared by plotting the hardness achieved for the different heat-treatment programs. With these results the program for the actual heat-treatment could then be decided.

3.2.2 Applying the found optimal heat-treatment program

After finding the best suited heat-treatment program all the rest of the plates could be heat treated as well. First 2-3 plates of each alloy was put in a Nabertherm N30/85HA Air circulation furnace, at a temperature of 535°C for 8 hours. Then after 8 hours all the plates was immediately quenched in water. After the quenching the artificial aging was next. Here the samples was put in a oil bath With silicon oil at 175°C for 8 hours. When this process was completed the samples was taken out of the oil bath and cooled in room temperature. Completing the heat-treatment process.

3.3 Material Testing

After the heat-treatment was completed various material test was completed. The tests that was completed was tensile tests, measuring the hardness, SEM, electrical conductivity and optical microscopy.

3.3.1 Tensile testing

In order to complete a tensile test on the heat treated sample they had to be machined into shapes suitable for this testing. Two plates from each alloys was then sent to the workshop here at NTNU where two tensile test samples was cut out for each plate giving four samples for each alloy. The shape of the machined samples can be seen in figure 3.3 and 3.4. The dimensions for the sample was can be seen in figure 3.5.

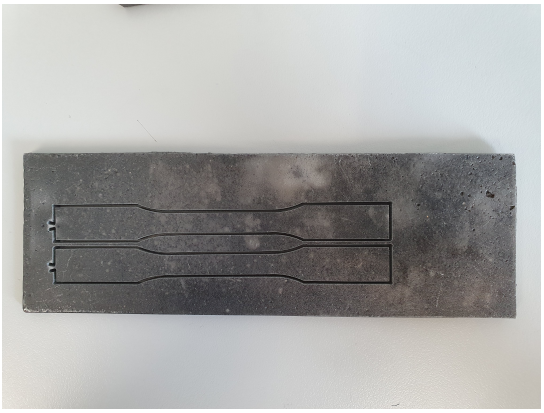

Figure 3.3: Machined tensile test samples, two samples for each plate.

Figure 3.4: Tensile test sample.

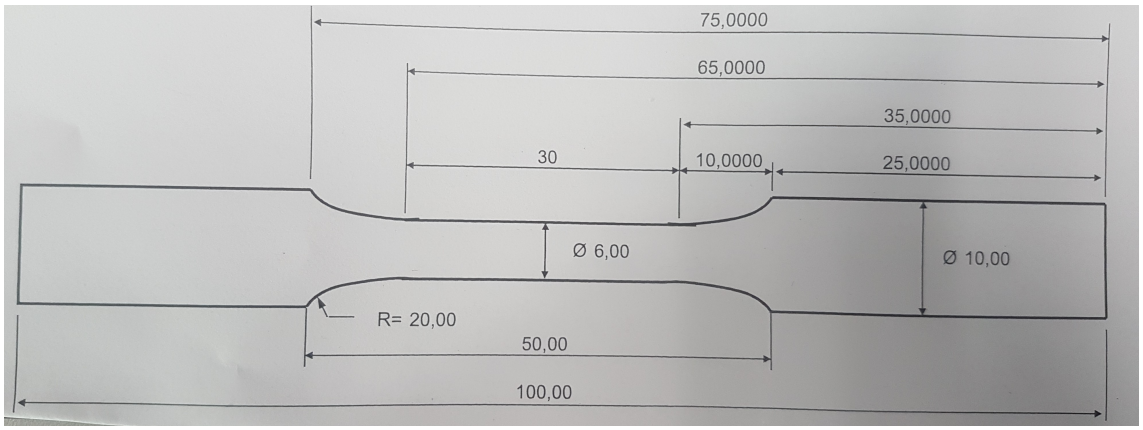

Figure 3.5: Dimensions for the sample that is used in for the tensile testing. All the values are given in mm.

After the machining was done the actual test was next in line. All the 20 samples was placed in a MTS 810 tensile test machine as figure 3.6 shows. The sample was then applied a uniaxially load, that increased consistently over time. The load increased all the way until the sample fractured. The machine then gathers information like the load, time, elongation, stress and strain that then can be used to calculate values like the yield strength and young's modulus.

Figure 3.6: Sample in a 110kN test machine[2].

3.3.2 Hardness

The testing of the hardness was done the same way as when the hardness was measured during the finding of right heat-treatment program. Meaning 1 sample

from each alloy was first selected to represent its alloy group, then they where polished into a nice smooth surface that would be easy to give an imprint. After the samples was polished they where tested in a Innovatest manual hardness testing machine, where the machine would take an imprint with a load of 1KN and by measuring the two diagonals of the imprint the hardness was calculated. This was done 10 times on each sample at different places on the surface so that an average hardness of the whole surface was measured. An example of the sample used is shown in figure 3.7.

Figure 3.7: Example of sample after polishing and ready for hardness testing.

3.3.3 Electrical conductivity

The electrical conductivity was tested by using a Sigmatest 2.069 as shown in figure 3.8. The probe that can be seen on the right side is placed on the plates, and the apparatus calculates the electrical conductivity in MS/m. This calculation was done on one plate for each alloy, with 8 tests for each plate. The average of each alloy was then calculated and plotted to illustrate the variation from alloy to alloy.

Figure 3.8: Sigmatest 2.069 apparatus used to calculate electrical conductivity.

3.3.4 Optical microscopy

As a further investigation into the story of each of the alloys, some of the samples was investigated in a optical microscope. Here the plates who had been heat treated was cut in the middle so that the cross-section appeared. This cross section was the desired area to investigate. After the cutting was completed on all the samples, they were all casted in epoxy so the sample preparation and polishing would be easier. After the solidification of the epoxy the samples was polished to a smooth surface, free of scratches. In order to have a good look at the grains in the aluminium alloy in an optical microscope, it is necessary to anodise the surface. This was done on all the sample using a Struers Lectropol-5 which sends 20V through the sample and the anodizing liquid of 5% HBF_4.

After the anodizing was completed the sample was ready for the optical microscope. There was then taken pictures of the prepared samples at various places. All the pictures were taken with 2.5x magnification, this was because it gave a better overview of how the grains distributed in the material. It also makes it easier and more accurate to calculate the average grain size when more grains can be measured in the same picture. The average grain size was then measured for each alloy, by using the method described in chapter 2.4.2. For each picture 10 lines was drawn with a length of 80mm.

3.3.5 Scanning Electron Microscope

As for the optical microscopy testing the cross section of the plates was examined in a Scanning Electron Microscope (SEM). This examination was done by Tomovic

Stanka Petrovic senior scientist at SINTEF Manufacturing. Firstly the samples was prepared and polished the same way as described in 3.3.4, but the samples was not anodized. After the sample preparation was completed new pictures was looked at in the optical microscope to see where one the sample it would be interesting to investigate further in the SEM. Pictures were taken here to showcase how the area that is investigated in the SEM appears. After a area is selected the sample is looked at in the SEM with back scatter electron (BSE). A mapping scan was conducted to investigate what elements that where present in the different phases and to get an overview of how the different elements have distributed in the sample. After the mapping different phases was discovered and to examine these further a EDS x-ray point analysis was conducted on selected phases. This analysis gave the total element composition in each of the phases tested. The mapping and the point analysis was done on the L1 and L5 alloys, representing each side of the scale. There was no point in doing the same with the other 3 as the tendency was already proven, and no new result would come from this.

Chapter 4

Experimental Results

In this chapter the results from the experimental work will be presented. All the results that have been gathered throughout this project will be put in this chapter or in the appendices. The results will not be discussed in this chapter.

4.1 Heat-treatment

When finding the optimal heat-treatment program the hardness was measured on different samples that had gone through different heat-treatment programs. The different parameters are given in table 3.3. In total there was taken 20 imprints and hardness measurements for each heat-treatment program. Table 4.1 shows the average value of all these 20 measurements, giving the hardness of the samples. All the measurements is given in the appendices in table A.1-A.6. A more visual representation is given in figure 4.1, where the average values is plotted and compared. The figure show that artifical aging at a temperature of 175°C gives the consistently highest hardness regardless of the holding time. However the holding time of 8 hours seems to give the best result. It is also worth noticing that the sample is held long enough at 160°C it will eventually get to the same values as for 175°C. Heating at 190°C seems to never reach the standards set by 175°C, and drops in hardness when held for a longer period of time.

Table 4.1: This table shows the average hardness of each of the samples for each heat-treatment program.

	2h [HV1]	4h [HV1]	8h [HV1]	16h HV1]
160°C	90.19	104.32	107.41	111.92
175°C	110.15	110.70	112.56	112.19
190°C	105.32	105.63	101.72	101.70

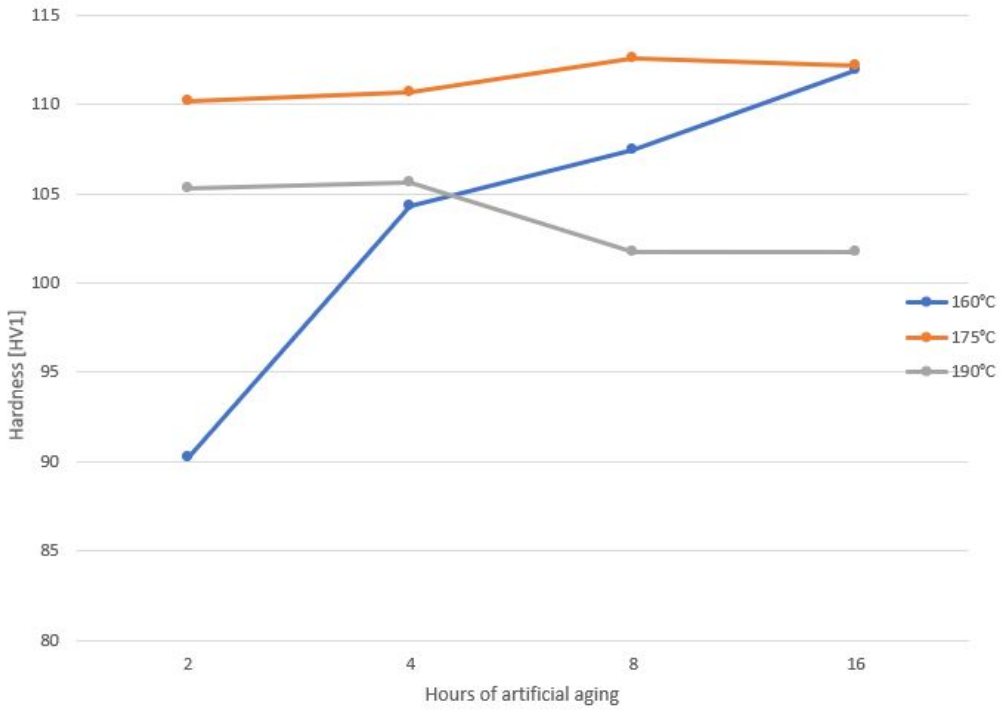

Figure 4.1: This figure gives a visual presentation of the average hardness values measured. The x-axis shows the hours of holding at the given temperature and the y-axis shows the hardness in HV1.

4.2 Tensile testing

The results from the tensile testing can be seen in the stress-strain plots in figure 4.2-4.5. Each colored line represent one of the four samples from each alloy.The slope of the elastic area and the Youngs modulus seems to be quite consistent internally for the alloys. But when the plastic deformation starts the samples seem to variate alot more, the point of fracture is very much different from sample to sample. This is the case for all the alloys. It is worth mentioning that some of the samples fractured outside of the scope of the extensometer, and will therefor be less accurate. This samples are the test 3 and 4 for L1, 2 and 3 for L3, 1 and 2 for L4 and test 2 and 4 for L5.

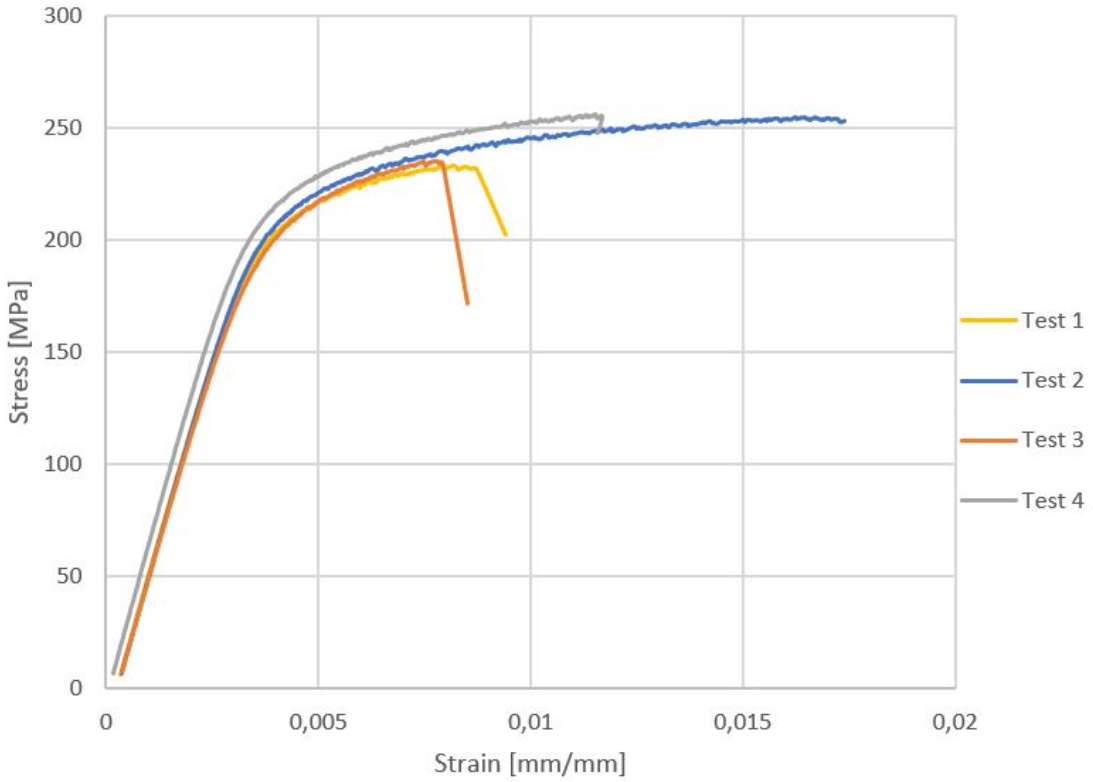

Figure 4.2: Stress-Strain plot of the 4 tests done for L1.

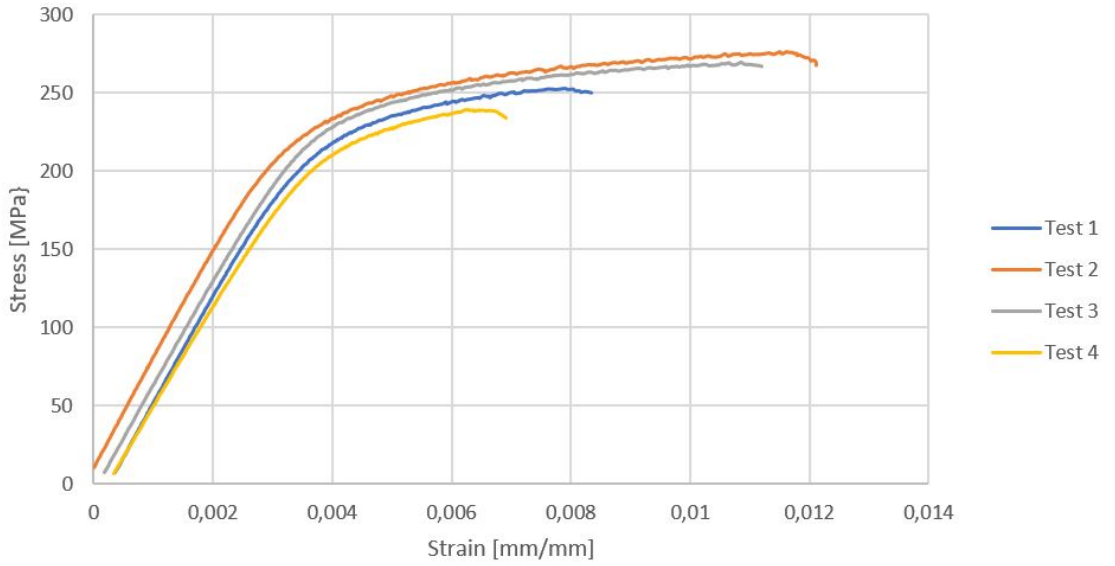

Figure 4.3: Stress-Strain plot of the 4 tests done for L2.

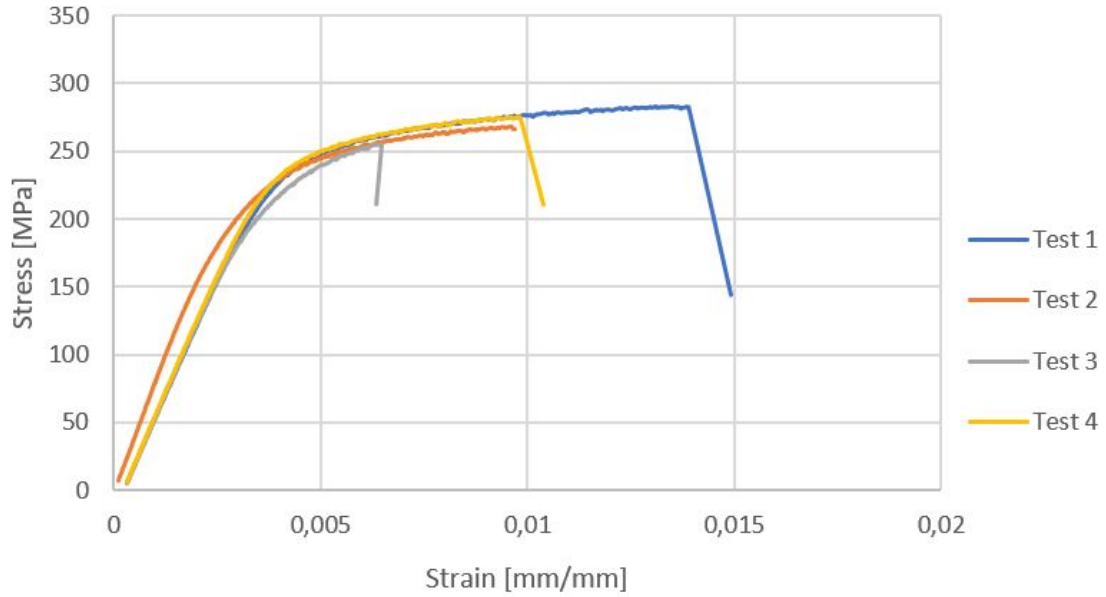

Figure 4.4: Stress-Strain plot of the 4 tests done for L3.

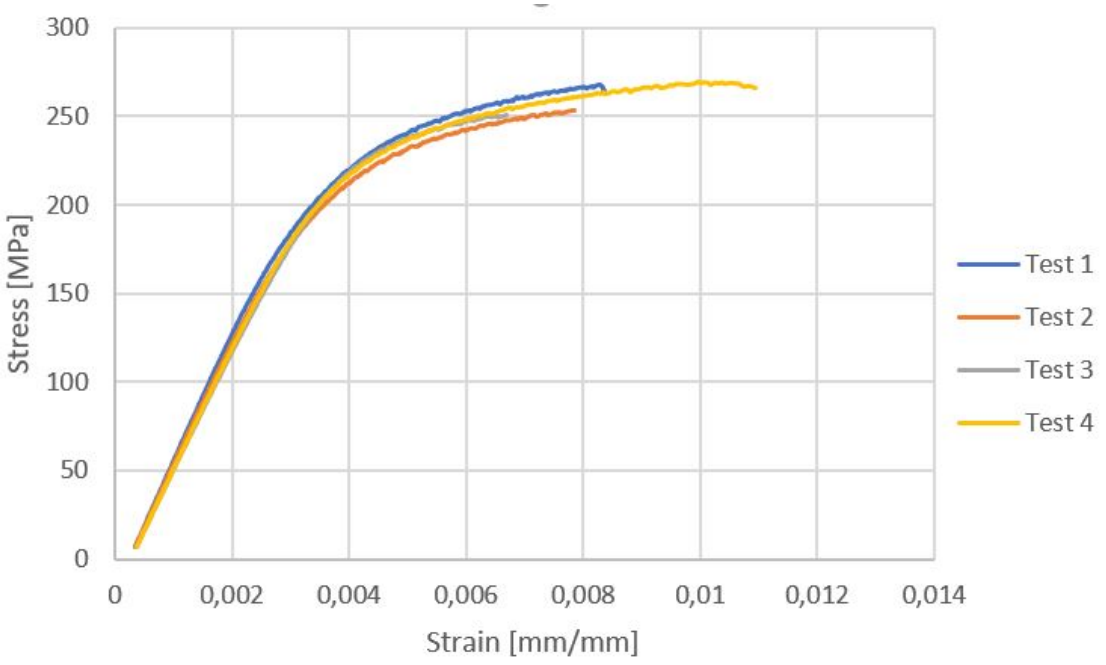

Figure 4.5: Stress-Strain plot of the 4 tests done for L4.

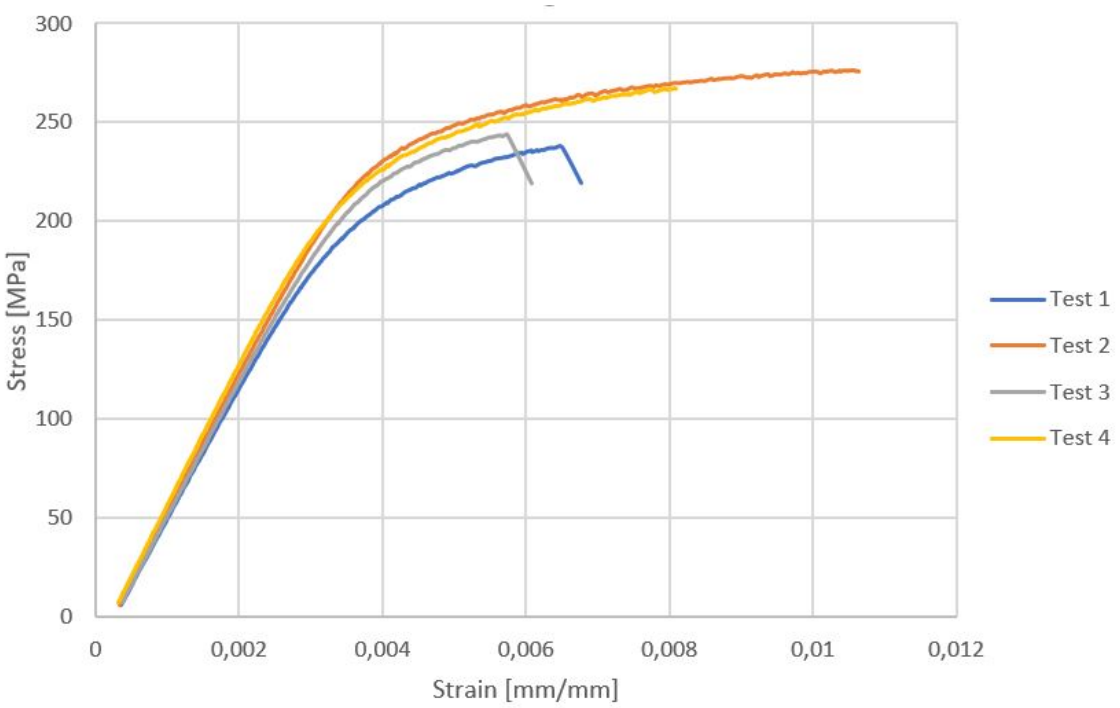

Figure 4.6: Stress-Strain plot of the 4 tests done for L5.

From the stress-strain plot different mechanical properties was calculated for each alloy. These values is presented in table 4.2, and is the average value of each of the four samples used in the testing. All the values used to calculate the average is presented in the appendix in table A.7-A.11. Here the trend seem to be that for the yield strength and UTS increases from L1 to L3 and then decreases from L3 to L5, making L3 the apex. For the E-modulus the value increases from L1 to L3 before it drops to L4 and then increases above the value of L3 at L5 making L5 the apex. It is worth mentioning that the E-modulus is an estimated value, for a completely accurate value, more testing is required. As for the strain at break L1 seems to have the highest value and L5 the lowest.

Table 4.2: Summary of the calculated average values from tensile testing for L1-L5.

	L1	L2	L3	L4	L5
Strain at break [%]	1.17	0.96	1.033	0.9	0.79
E-Modulus [GPa]	61.55	63.53	64.83	62.38	65.15
Tensile stress at maximum load [MPa]	244.73	259.58	270.23	260.43	256.35
Tensile stress at yield [MPa]	22.,13	246.08	259.55	251.15	246.93

4.3 Hardness for heat treated alloys

All the values measured during the hardness testing of the heat treated alloys is given in table 4.3. With an average value calculated at the bottom. This average is used to plot the hardness of the different alloys to compare them to each other, this plot is given in figure 4.7. Here you can easily see that the hardness variate from alloy to alloy, and L4 has the highest value while L1 has the lowest. The plot

does not have a uniform incline where it increases from L1 to L2 to L3 and so on, it changes from alloy to alloy. However it does show that L4 and L5 has a higher hardness value than the other 3 alloys.

Table 4.3: Results from hardness testing done after heat-treatment on all the different alloys.

	L1 [HV1]	L2 [HV1]	L3 [HV1]	L4 [HV1]	L5 [HV1]
1	103.1	111.3	110.9	106.7	113.4
2	106.7	114.0	112.0	104.9	113.5
3	105.3	104.7	101.0	114.3	116.7
4	109.7	110.5	109.9	116.7	105.7
5	111.2	112.1	103.8	107.3	99.2
6	106.5	107.2	112.0	112.1	107.4
7	106.9	107.6	104.6	107.3	101.1
8	109.6	102.2	106.8	114.9	113.9
9	102.6	105.4	108.0	114.5	112.7
10	101.5	106.4	105.2	110.5	116.1
Average	106.3	108.1	107.4	110.9	110.0

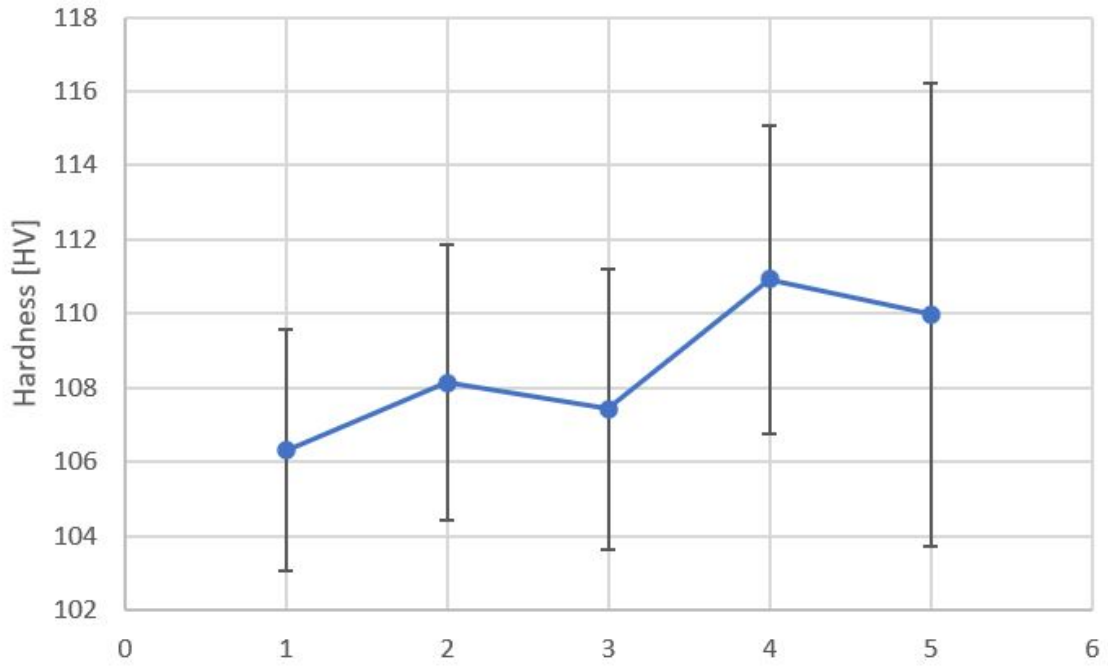

Figure 4.7: Plot that visualises the hardness of each alloy and how they compare to each other. The x-axis represent the different alloys where 1 is L1 and so on. The y-axis is the average hardness in HV1.

4.4 Optical Microscope

The pictures taken with the optical microscope of the anodized samples is shown in figure 4.8 to 4.12. These figures is from alloy L1 to L5 and shows how the grain structure variate for the different composition. There was taken different pictures for each alloy at different places, these are given in the appendix in figure A.1a to A.5b. All the pictures is taken with a 2.5x magnification lens.

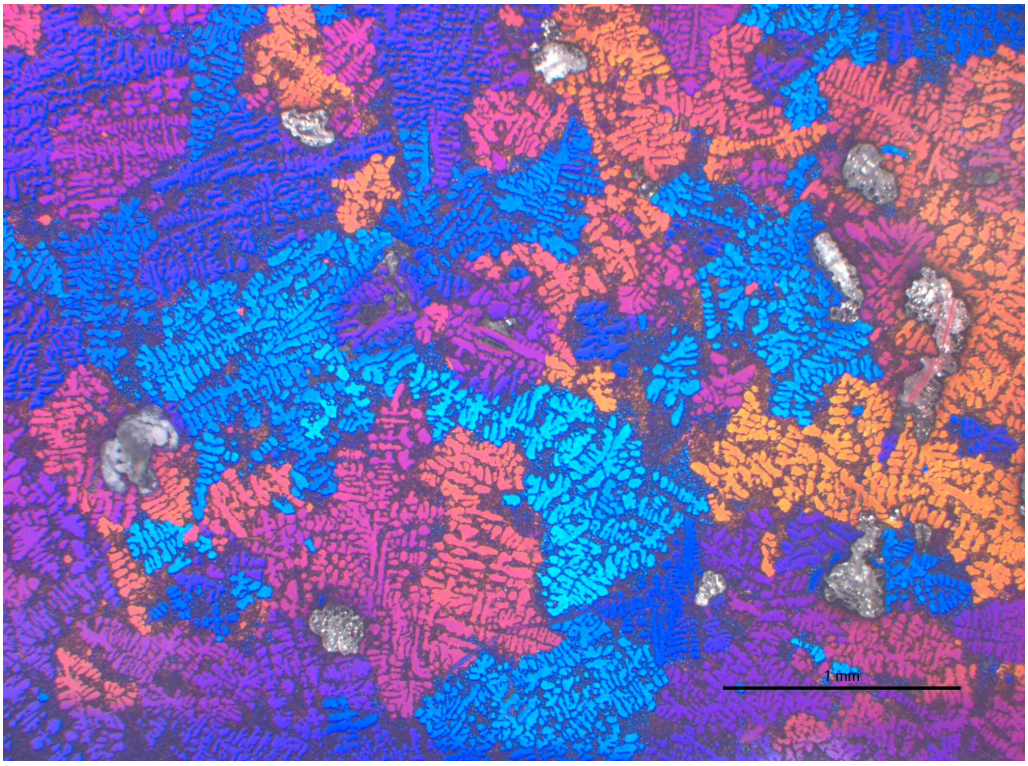

Figure 4.8: Optical microscope picture of anodized cross-section of plate from the L1 alloy. The picture is taken with a 2.5x magnification lens.

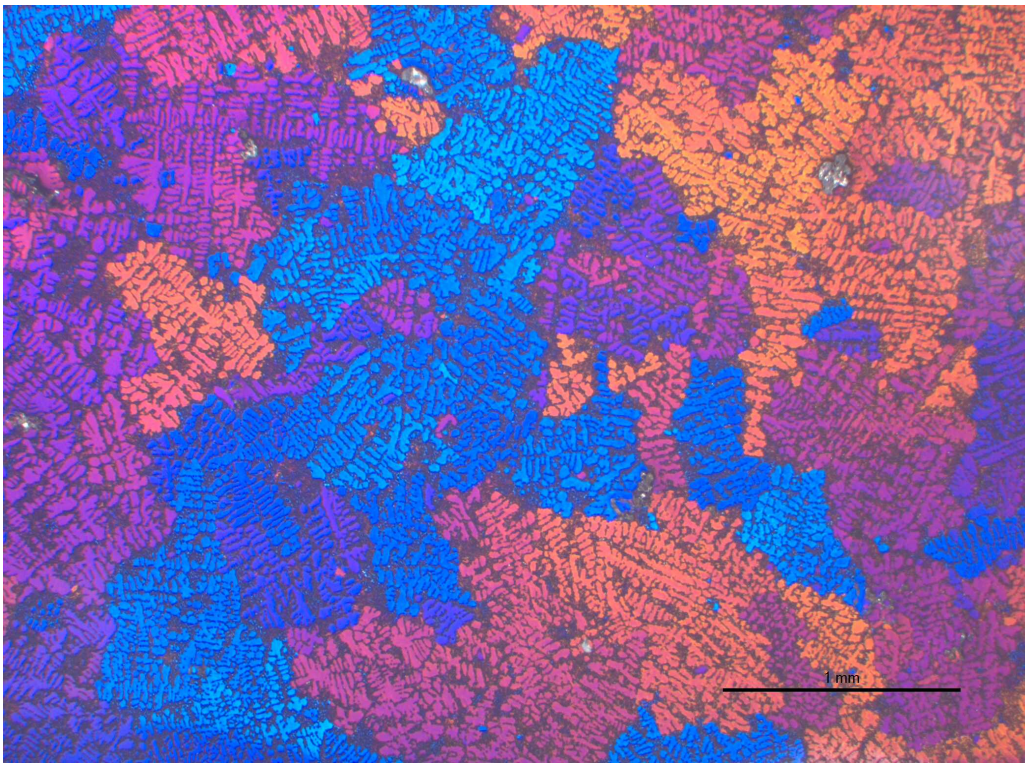

Figure 4.9: Optical microscope picture of anodized cross-section of plate from the L2 alloy. The picture is taken with a 2.5x magnification lens.

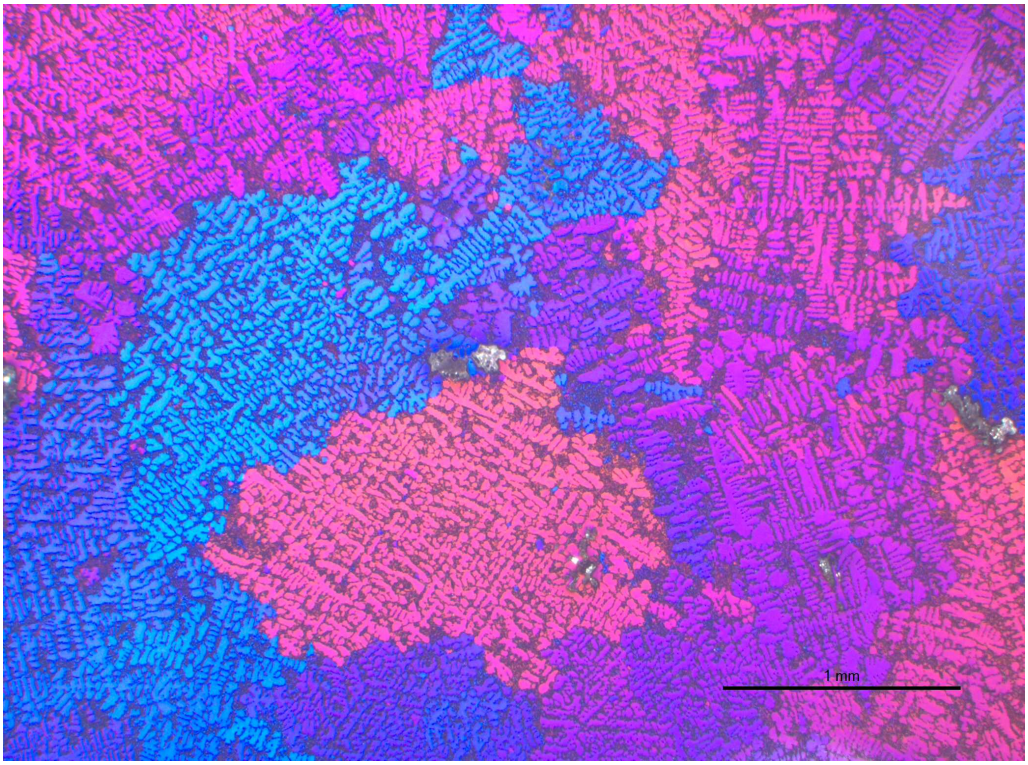

Figure 4.10: Optical microscope picture of anodized cross-section of plate from the L3 alloy. The picture is taken with a 2.5x magnification lens.

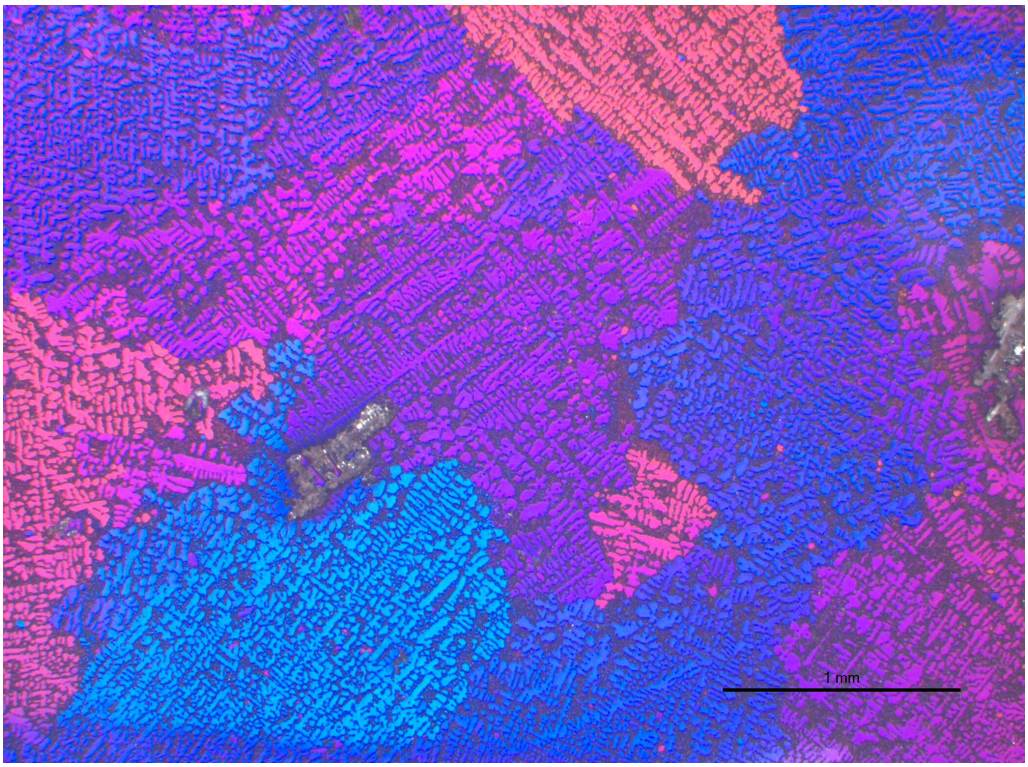

Figure 4.11: Optical microscope picture of anodized cross-section of plate from the L4 alloy. The picture is taken with a 2.5x magnification lens.

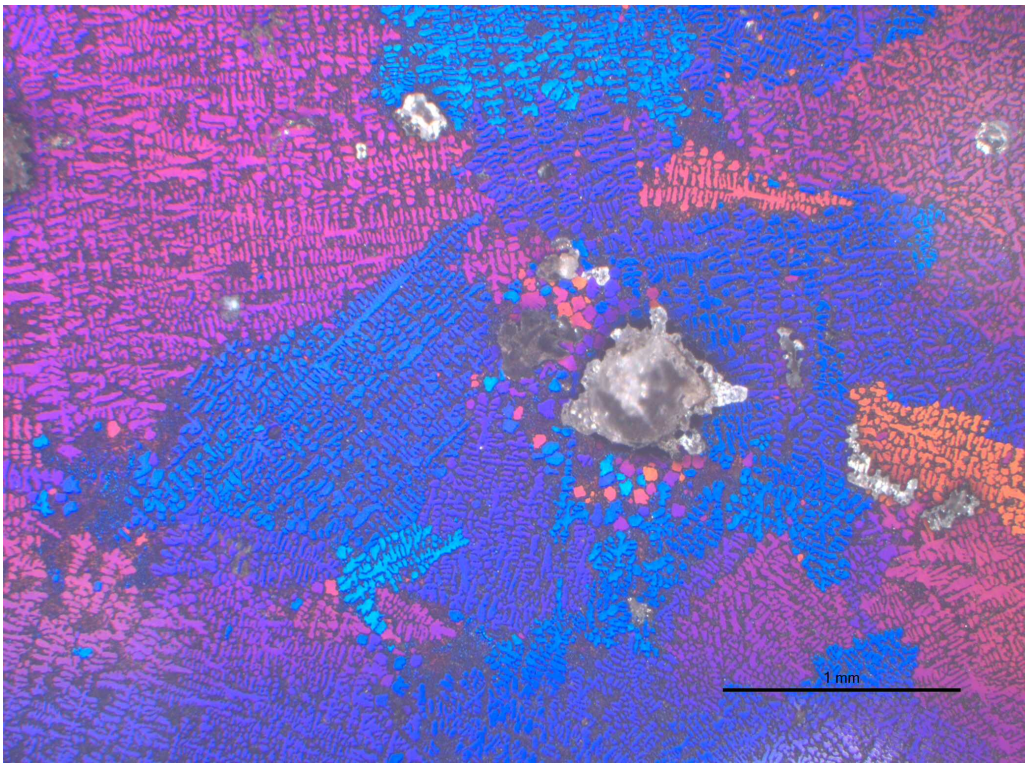

Figure 4.12: Optical microscope picture of anodized cross-section of plate from the L5 alloy. The picture is taken with a 2.5x magnification lens.

Since the surface of the sample is anodized, the grains is easy to see. It is there-

fore possible to calculate a average grain size for each alloy. The results from this calculation is given in table 4.4 and figure 4.13. The table shows that the average grain size can variate quite a lot within the alloy where for L5 the value calculated form one picture can be 0,66mm and for another picture it can be 0,48mm, proving that the grain size is irregular. Figure 4.13 show a plot of the calculated average grain size in each alloy. The plot illustrates how the grain size variate from alloy to alloy, increasing gradually from L1 to L3 before decreasing gradually from L3 to L5 making L3 the apex.

Table 4.4: Calculations of average grain size. Each of the alloys where calculated 3 times with 3 different pictures. The average of this is the average grain size of the alloy, given at the bottom of the table.

	L1 [mm]	L2 [mm]	L3 [mm]	L4 [mm]	L5 [mm]
1	0.45	0.44	0.76	0.6	0.55
2	0.34	0.46	0.63	0.66	0.66
3	0.46	0.5	0.73	0.72	0.48
Average	0.42	0.47	0.71	0.66	0.56

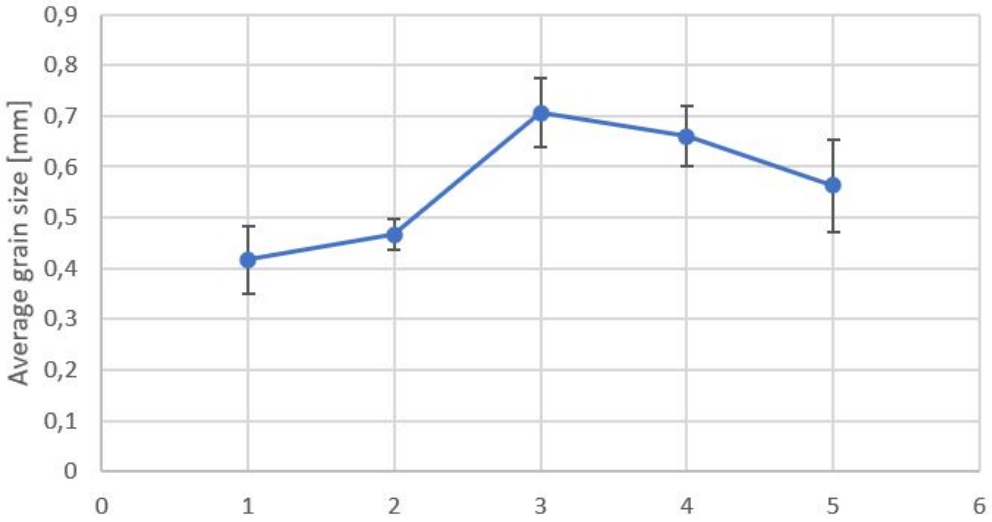

Figure 4.13: Plot of the average grain size of each alloy, that illustrate how the grain size variate from alloy to alloy.

4.5 Scanning Electron Microscope

All the results from the SEM is given in this chapter. The testing was done on L1 and L5 as mentioned in chapter 3.3.5, with the mapping and EDS point analysis giving the main results. The results from the L1 and L5 is presented separately in chapter 4.5.1 and 4.5.2 respectively, before a summary and comparison of the two is given in chapter 4.5.3.

4.5.1 SEM results for L1

The mapping of the L1 sample was done in the area represented by the pink square in figure 4.14. The result from this mapping is given if figure 4.15-4.18. This mapping shows which phases are located where. The mapping shows that as expected the aluminium is dominating the sample with silicon, iron and magnesium also represented to some extent. The mapping also detected some areas where strontium, phosphorous, calcium and manganese appeared.

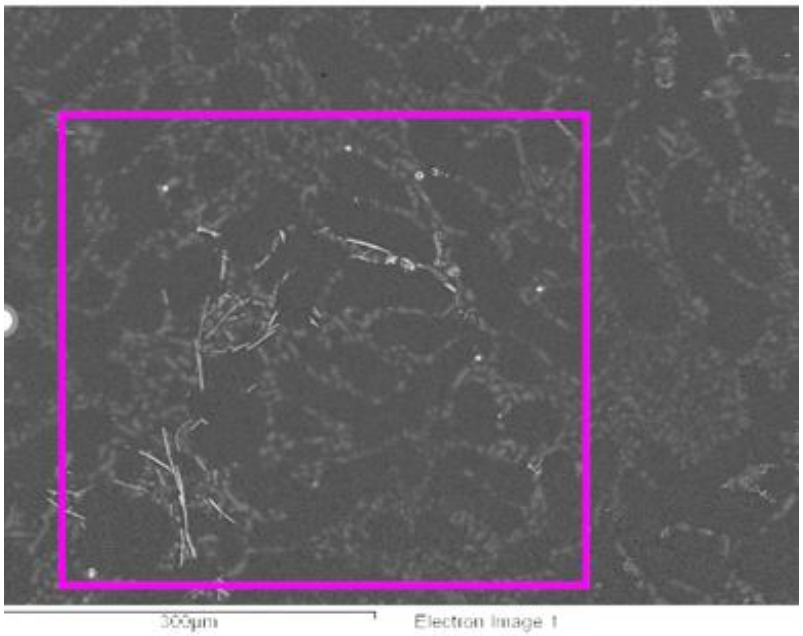

Figure 4.14: Picture taken with SEM that illustrates the area where the mapping was conducted on the L1 alloy. The area inside the pink square was investigated.

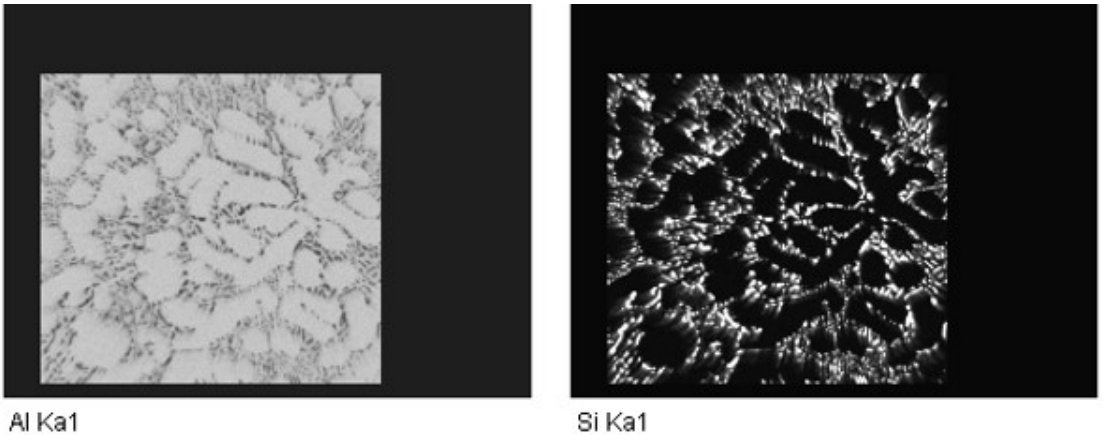

(a) (b)

Figure 4.15: Results from mapping done on the L1 alloy. (a) shows the detection of aluminium while (b) shows the detection of silicon.

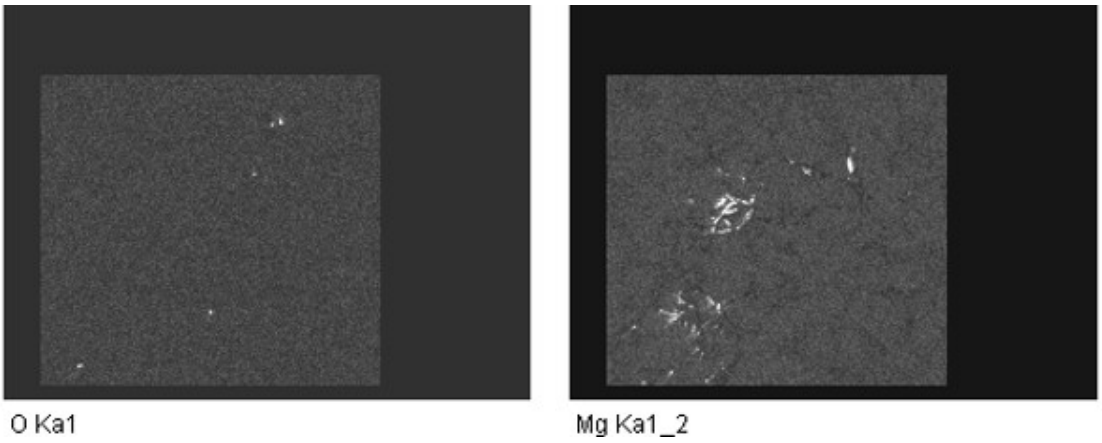

(a) (b)

Figure 4.16: Results from mapping done on the L1 alloy. (a) shows the detection of oxygen while (b) shows the detection of magnesium.

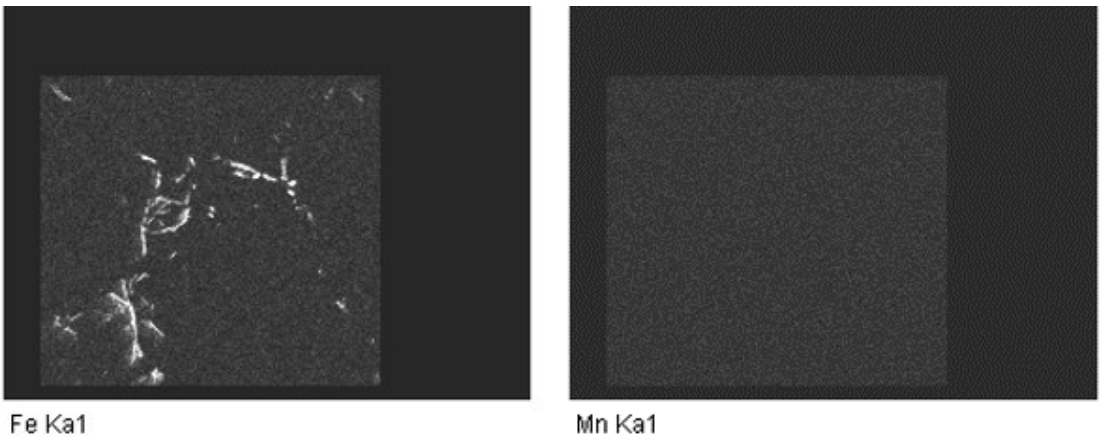

(a) (b)

Figure 4.17: Results from mapping done on the L1 alloy. (a) shows the detection of iron while (b) shows the detection of manganese.

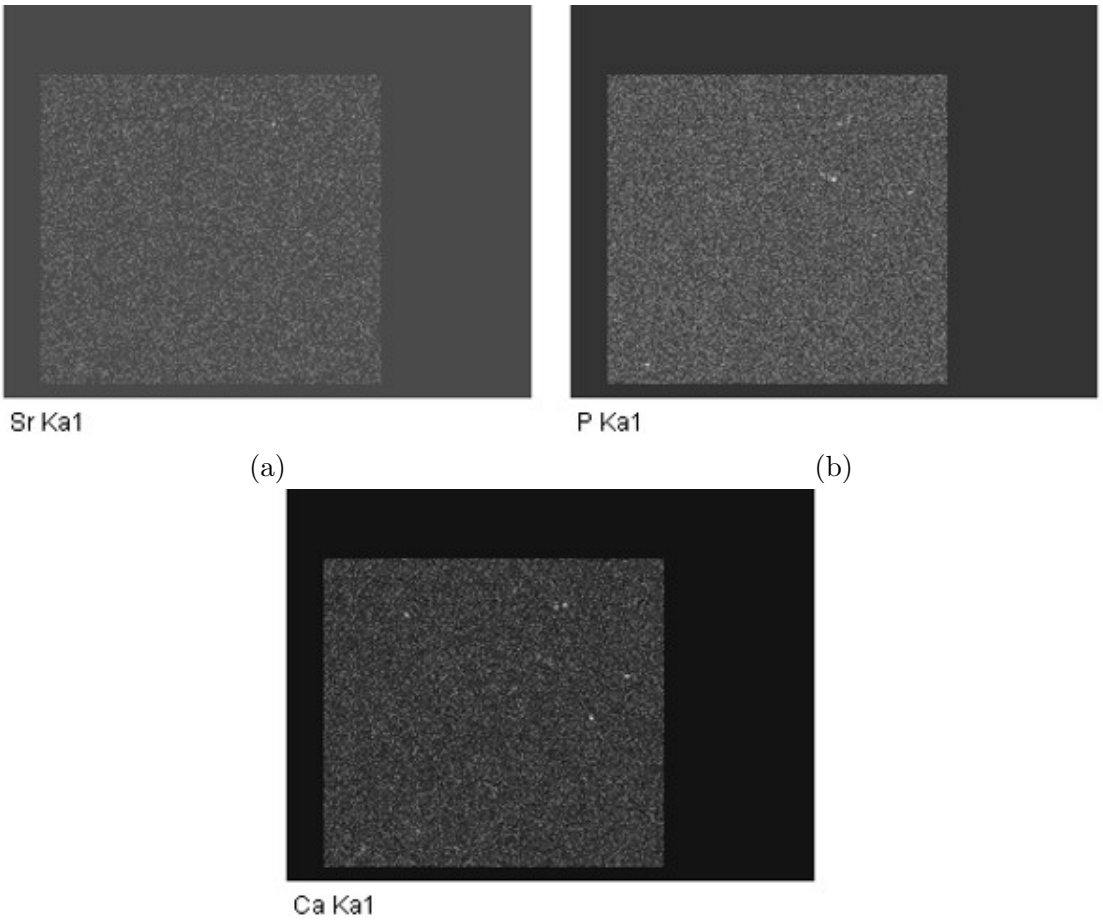

(a) (b)

(c)

Figure 4.18: Results from mapping done on the L1 alloy. (a) shows the detection of strontium, (b) shows the detection of phosphorous and (c) shows the detection of calcium.

The mapping gave interesting areas to investigate with EDS point analysis, figure 4.19 shows at which phases the different point analysis where taken. The point analysis then gave the chemical composition in each point. This result is presented in table 4.5. Here 5 different phases found in the sample are presented, the aluminium matrix with approximately 97.6% aluminium, a silicon based phase, a iron baring phase, a strontium baring phase and an AlSiFeMg phase.

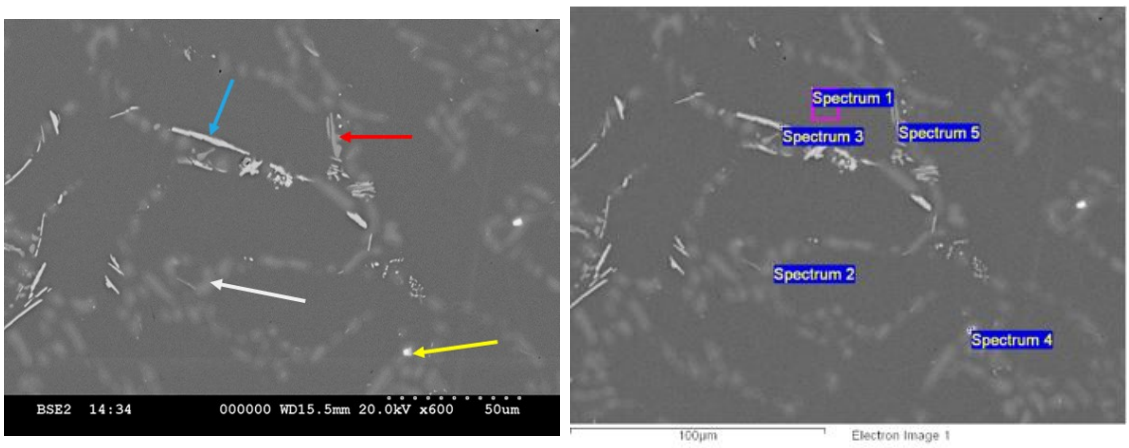

(a) (b)

Figure 4.19: Visual representation of where the point analysis is taken. The arrows in (a) points to the places where the different point analyses is taken. Spectrum 1 is in the aluminium matrix in is visualised with the pink square in (b), spectrum 2 is the white arrow, spectrum 3 is the blue, spectrum 4 is the yellow and spectrum 5 is the red arrow.

Table 4.5: Results from the EDS point analysis for L5. The table shows how much of each element is found in the different phases.

Spectrum	O	Mg	Al	Si	Ca	Mn	Fe	Ni	Sr	Total	Comment
1	0.7	0.5	97.6	1.1			0.1		0.0	100.0	Matrix
2			16.3	83.7						100.0	Silicon based phase
3		0.2	80.1			0.3	19.2	0.2		100.0	Iron baring phase
4	0.7	1.7	28.0	44.4	1.9				23.3	100.0	Strontium baring phase
5		12.5	55.1	23.2			9.1			100.0	AlSiFeMg phase

4.5.2 SEM results for L5

The mapping of the L5 alloy was done in the area represented by the pink square in figure 4.20. The result from this mapping is given if figure 4.21-4.26. This mapping shows which phases are located where. The mapping shows that as expected the aluminium is dominating the sample with silicon, iron, magnesium, oxygen and manganese also represented to some extent. The mapping also detected some areas where strontium, phosphorous, calcium, copper, nickel and zinc appeared.

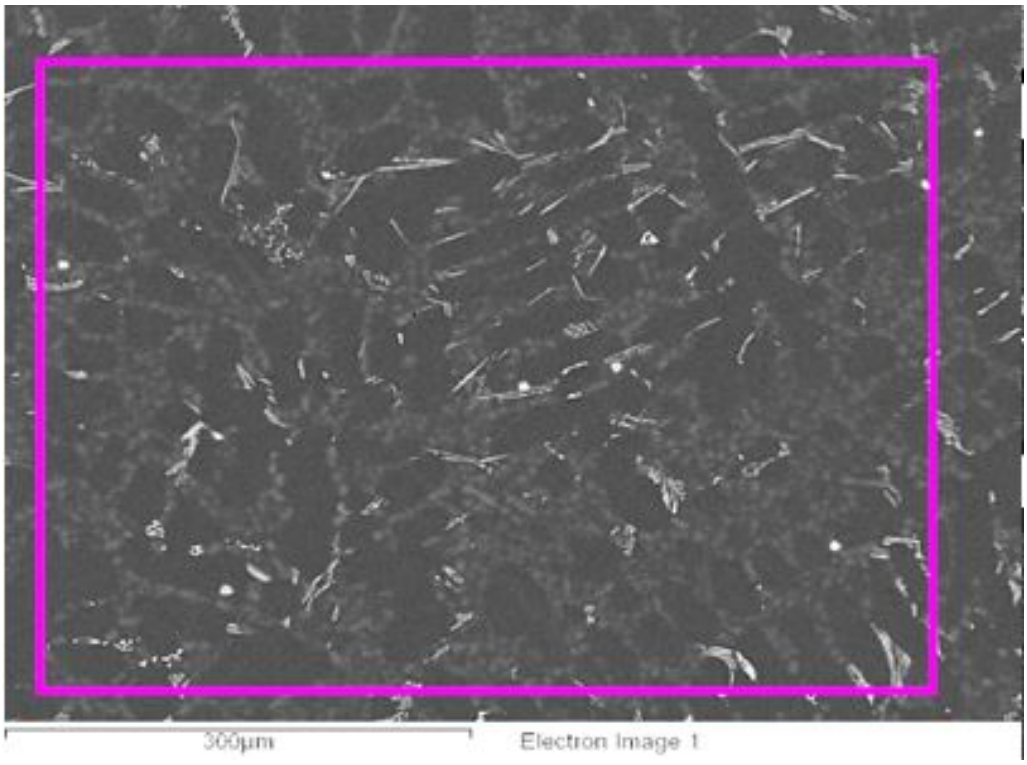

Figure 4.20: Picture taken with SEM that illustrates the area where the mapping was conducted on the L5 alloy. The area inside the pink square was investigated.

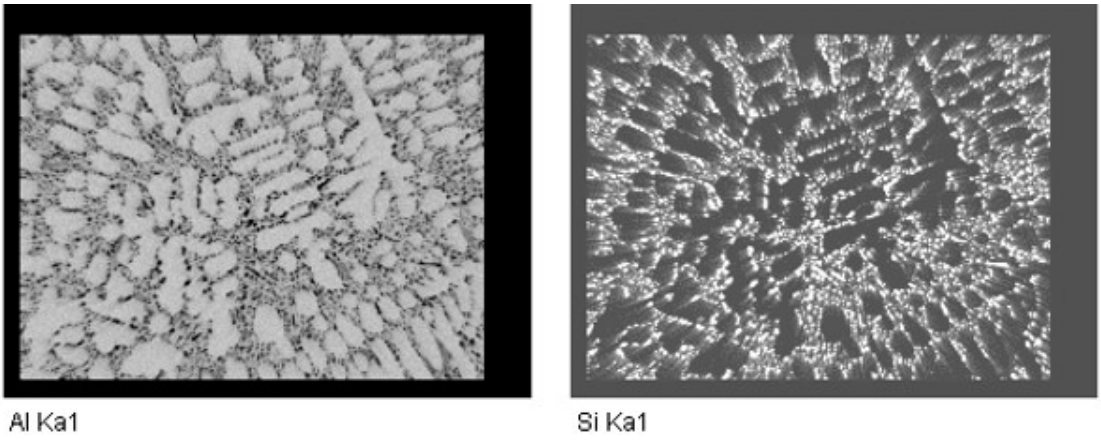

(a) (b)

Figure 4.21: Results from mapping done on the L5 alloy. (a) shows the detection of aluminium while (b) shows the detection of silicon.

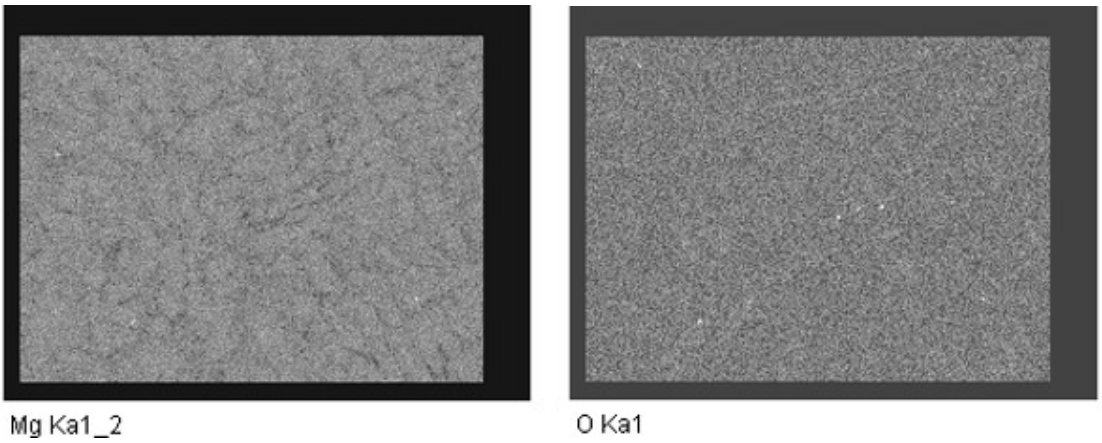

(a) (b)

Figure 4.22: Results from mapping done on the L5 alloy. (a) shows the detection of magnesium while (b) shows the detection of oxygen.

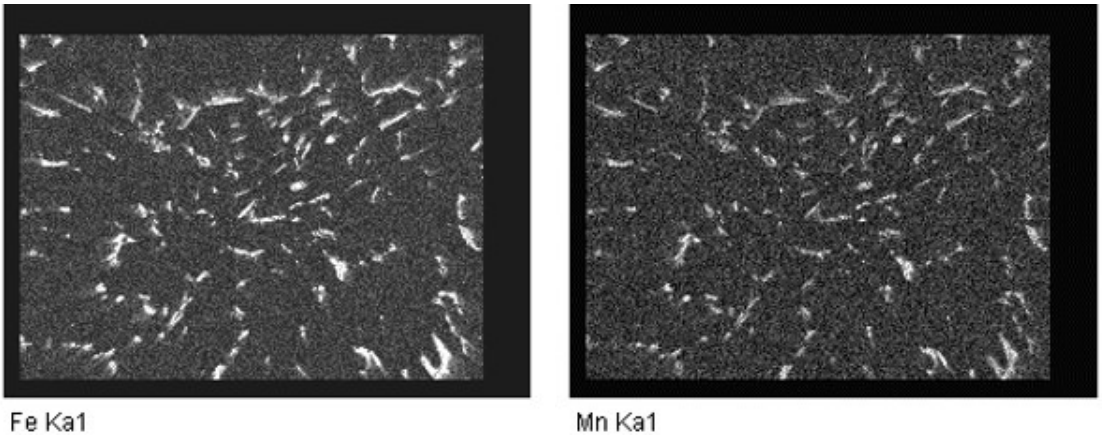

(a) (b)

Figure 4.23: Results from mapping done on the L5 alloy. (a) shows the detection of iron while (b) shows the detection of Manganese.

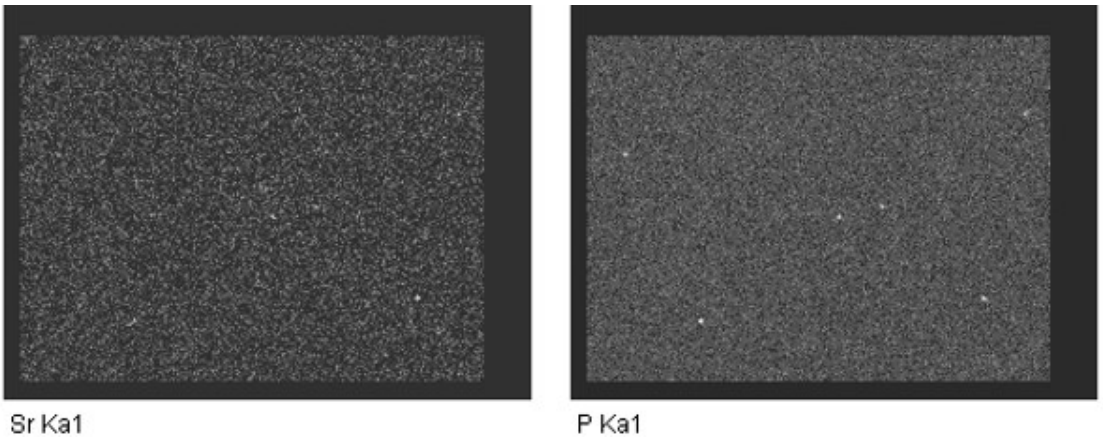

(a) (b)

Figure 4.24: Results from mapping done on the L5 alloy. (a) shows the detection of strontium while (b) shows the detection of phosphorous.

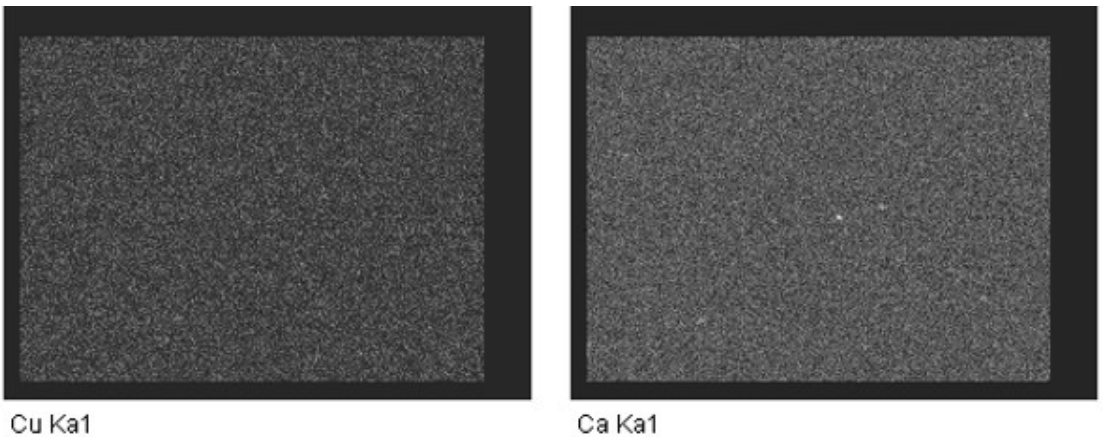

(a) (b)

Figure 4.25: Results from mapping done on the L5 alloy. (a) shows the detection of copper while (b) shows the detection of calcium.

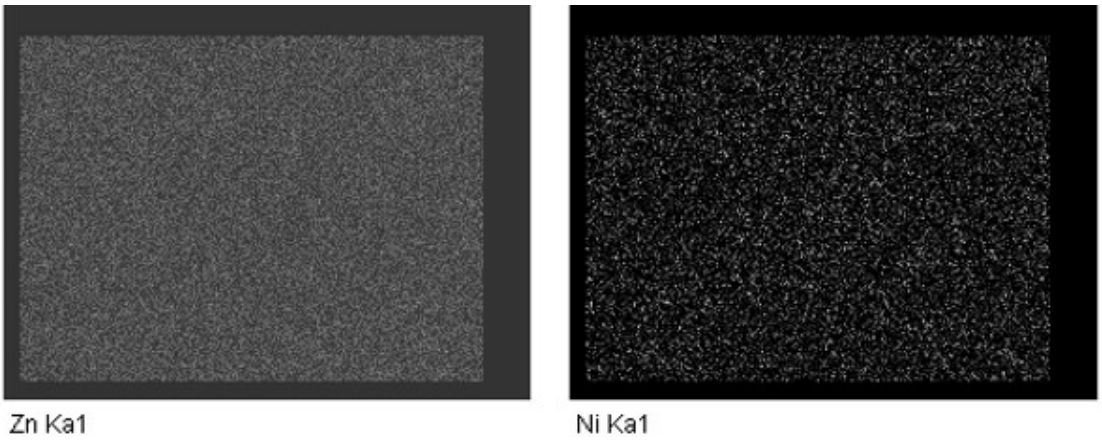

(a) (b)

Figure 4.26: Results from mapping done on the L5 alloy. (a) shows the detection of zinc while (b) shows the detection of nickel.

The mapping gave interesting areas to investigate with EDS point analysis, figure 4.27 shows at which phases the different point analysis where taken. The point analysis then gave the chemical composition in each point. This result is presented in table 4.6. Here there is presented 9 different spectrum where 1 and 6 is the results for the aluminium matrix, 2 is the silicon phase, 3,6,7,8 and 9 show a AlFeMnSi phase and 4 shows a strontium baring phase.

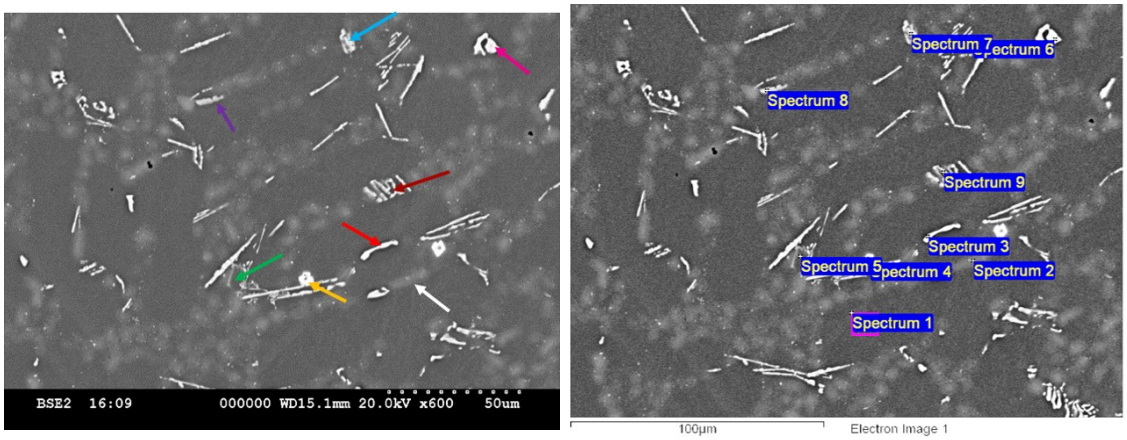

(a) (b)

Figure 4.27: Visual representation of where the point analysis is taken. The arrows in (a) points to the places where the different point analyses is taken. Spectrum 1 is in the aluminium matrix in is visualised with the pink square in (b), spectrum 2 is the white arrow, spectrum 3 is the red, spectrum 4 is the yellow, spectrum 5 is the green arrow, spectrum 6 is the pink, spectrum 7 is the blue, spectrum 8 is the violet and spectrum 9 is the brown arrow.

Table 4.6: Results from the EDS point analysis for L5. The table shows how much of each element is found in the different phases.

Spectrum	O	Na	Mg	Al	Si	P	Cl	Ca	V	Mn	Fe	Cu	Zn	Sr	Total	Comments
1	0.7		0.4	97.4	1.0					0.1	0.1	0.2	0.2		100.0	Matrix
2	0.5		0.2	35.6	62.7					0.2	0.1		0.1	0.6	100.0	Silicon
3			0.2	69.7	8.7					9.9	11.0	0.4	0.1	0.1	100.0	AlFeMnSi phase
4	13.5		2.0	34.6	18.2	3.6	0.2	1.4		0.1	0.6			25.9	100.0	Strontium bearing phase
5	0.7		0.4	92.0	4.2					0.8	1.6	0.1		0.2	100.0	Matrix
6		0.3	0.1	62.1	9.2		0.3		0.4	10.7	16.5	0.5			100.0	AlFeMnSi phase
7			0.3	75.0	8.1					4.8	11.6	0.3	0.1		100.0	AlFeMnSi phase
8			0.4	85.2	4.9					2.9	6.3	0.2	0.2		100.0	AlFeMnSi phase
9	0.8		0.3	83.3	3.8					3.3	8.3	0.2	0.1		100.0	AlFeMnSi phase

4.5.3 Summary of SEM results

Comparing the SEM results from L1 and L5 comes up with some interesting results. First of all the Mapping detected more elements for L5 than for L1, like zinc and copper. Further testing with the EDS point analysis showed the change from an AlFeSiMg phase in L1 to a AlFeSiMn phase for L5, where the magnesium seem to have segregate, and is spread throughout. The iron phases seem to go from being more clustered together to being more spread out throughout the alloy from L1 to L5.

For the strontium-baring phase the amount of silicon has gone from approximately 44.4% to only 18.2%, and also detecting some that was not detected in L1 like phosphorous and chlorine. As for the aluminium matrix and the silicon phase, both seem to be somewhat similar in L1 and L5.

4.6 Electrical conductivity

A sigmatest was completed to calculate and compare the electrical conductivity of the different alloys. the results from this test is given in table , where all the values from the testing is gathered. Then a more visual representation of the results and the average value of each alloy is presented in figure . This figure shows that with all most all the error overlapping each other the electrical conductivity does not variate significantly between the alloys.

Table 4.7: Results from the sigmatest for all the alloys given in MS/m.

	L1 [MS/m]	L2 [MS/m]	L3 [MS/m]	L4 [MS/m]	L5 [MS/m]
1	22.68	22.38	22.22	21.84	21.63
2	21.52	22.01	22.16	21.96	21.46
3	21.78	22.29	22.20	21.98	21.37
4	22.45	22.51	21.93	21.74	21.38
5	22.77	22.22	22.10	21.83	21.59
6	22.72	22.24	22.13	21.89	21.76
7	21.46	21.81	22.27	21.84	21.38
8	22.55	21.59	22.12	22.01	20.26
Average	22.24	22.13	22.14	21.89	21.35

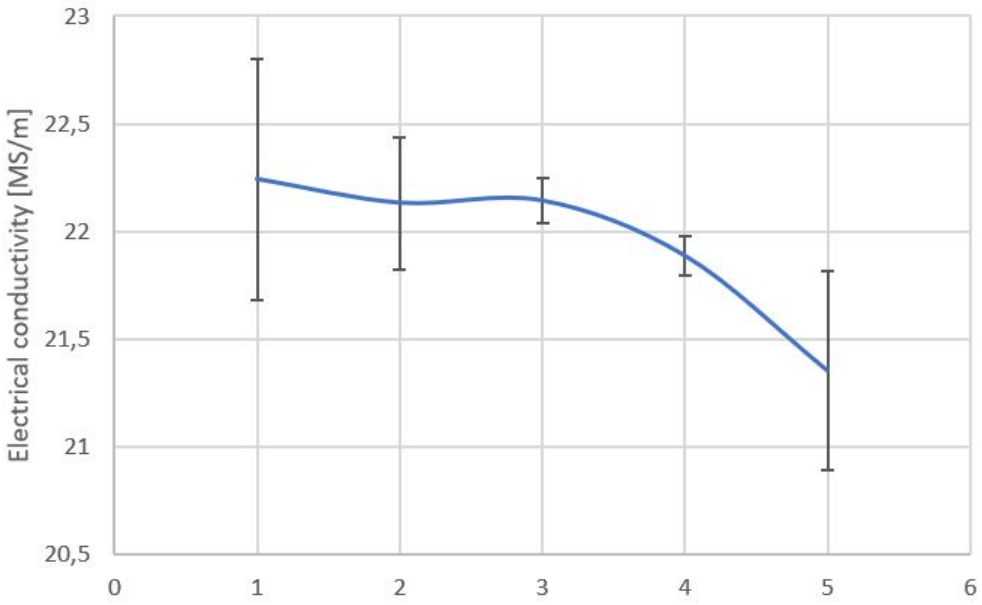

Figure 4.28: Plot of the average value of the electrical conductivity for all the 5 alloys.

Chapter 5

Discussion

In this chapter all of the results done in this project will be discussed. The different results will first be discussed separately in separate sub chapters, before a summary of all the results will be discussed.

5.1 Finding the optimal heat-treatment program

The first thing that was done during the work on this master thesis was finding a optimal heat-treatment program for the casted plates from the work done last semester. Since Hydro had completed a simulation on a heat-treatment program on the alloy, most of the variables was know to some degree. The solution heat-treatment was decided from the simulation and based on how NORSE metal conducted their heat-treatment that this would be done at 535°C for 8h. So the only variable that needed testing was the artificial aging. The result from the hardness test done after testing the different artificial aging temperatures gave results that would help in picking the right heat-treatment program. The choice ended eventually on 175°C for 8h, this was the result Hydro had gotten the best values from their simulation and also the result that was best for the hardness test done in this thesis.

The hardness result is the average value so the standard deviation does overlap in some of programs, but since 175°C was the most stable out off all the temperature ranges, it was clear that this was the right temperature for this alloy. As for the choice of aging time, all the hours was quite similar. Here the simulation done by Hydro was the convincing factor, for their simulation the curve flattened out after 8h of aging. Ageing it longer would probably not make it worse, but not significantly better either. So the most cost, time and strength efficient way is to age for 8 hours.

The heat-treatment testing was only done for the L1 alloy, meaning that the optimal program for each alloy was not investigated as accurate. However it is reasonable to believe that it would not have been massive differences in results using other alloys. A complete and bigger investigating into various heat-treatment program for all the alloys would be recommend for further research. For the work done in this thesis, it would be less relevant. It would be much more time consuming and the comparisons

between the alloys would be less relevant.

5.2 Tensile testing

The first thing that is noticeable when looking at the stress-strain curves from the tensile testing, is that for each of the alloys the different test seem to variate when it comes to the plastic part and where the fracture happened. While the elastic part and the Young's modulus seem to be somewhat the same. The difference observed in the plastic zone can come from a number of reasons, but the most likely one is the presence of defects. More accurately the large number of pores found in the casted products. The pores will advance the crack propagation and therefor result in an earlier fracture, compared to a defect free material. Since these pores in the metal is found spontaneously and random, the fractures will variate from sample to sample.

Another factor that could be partly responsible for this variation, is the fact that 8 of the samples fracture outside of the exstensometer. This means that the machine did not register the fracture completely, so the results will therefor not be completely accurate. However the reason behind this could also be the pores, if the sample has large pores outside of the extensometer area and less pores inside there could be possible for the fracture to occur outside the area. But the most likely reason behind this error is poor machining of the samples.

It is not only a difference within each alloy it is also a noticeable difference between alloys. As table 4.2 shows the values of strain at break, Young's modulus, UTS and yield strength variate from alloy to alloy. Overall L3 seems to have the most consistently high properties, where the trend is an increase from L1 to L3 and a decrease from L3 to L5. The reasoning behind this is most likely the chemical composition, where the alloying elements added has had an effect on the mechanical properties of the alloy. This proves that the addition of more recycled aluminium can have a positive effect on the mechanical properties, but adding to much can worsen the properties.

By comparing the results from the tensile testing done in the project work, a few interesting points can me made. First of all it is worth stating that the heat-treatment conducted on the samples in this thesis work has had an positive effect, where it has increased the yield strength and UTS significantly, but the ductility have decreased for all these alloys. This means that the heat-treatment of the alloys comes at a price, a much greater strength will make the material more brittle.

Another point is that the observation done within each alloy both before and after the heat-treatment, is the same. Meaning that the heat-treatment has, as expected, not done anything with the porosity of the sample. The samples are still breaking at different stages within each alloy. The difference is that they can withstand higher force before fracture. It is also further confirming the statement that the inconsistency is due to the porosity, since the heat-treatment doesn't effect the porosity. The same trend comparing the different alloys also is relatively similar for the heat treated alloys and the as-cast samples substantiating that addition of recycled aluminium can increase the mechanical properties, but adding to much can have a

negative effect.

5.3 Hardness testing

The results from the hardness testing can not prove that the effect of the alloying elements has a big influence on the hardness. The graph in figure 4.1 shows some variation from alloy to alloy, however when measuring the hardness many imprints is taken at random places on the surface. The hardness in these places can variate on each sample. This variation is illustrated with the error bars in the figure, and shows that they overlap for each alloy. Meaning that the effect the alloying elements has had is minimal.

5.4 Optical microscope

The results from the optical microscope showed the grain structure and how the grain size variate from alloy to alloy. The first noticeable observation from the pictures taken with the OM is that for all the alloys the grains seem to be fine grained. When the average grain size was calculated the smallest size was the L1 alloy at 0.42mm, which is acceptable for industry use. The average grain size results showed that the grain size variate from alloy to alloy, proving that the addition of the alloying elements has an effect on the grain size of the alloy. With L3 having the larges average grain size. The reasoning behind this variation could be that the addition of the alloying elements has changed the solidification temperature, making the solidification variate. A slower solidification rate will result in larger grains, and "vice versa". Since the dendritic arm length seem to be the same for the various grains, the solidification conditions seem to be the same. Which may indicate that the nucleation is the cause of the difference in grain size.

Comparing the results from the project work where the grains where looked at without the heat-treatment. The tendency is somewhat the same, with an increase in grain size form L1 to L3, and a decrease from L3 to L5. This proves that the heat-treatment has not effected the various alloys differently.

5.5 Scanning electron microscope

The main differences spotted between the L1 and L5 alloy is how the Fe, Mn and Mg behave. The iron goes from being clustered in L1 to more spread in L5 out throughout the sample and in a higher quantity. This can be explained due to the fact that more iron has been added in the L5 alloy giving more phases. The manganese goes from being almost undetectable to being found in a higher quantity in phases at various places in the L5. This indicates that the Mn has attached and formed a phases with other elements in a larger scale than for L1. The magnesium has also changed where in L1 the Mg was found in various phases in the sample, but in L5 it is dissolved into the sample and not found in a specific amount of phases.

For L1 the Mg seem to follow the iron phase, but for L5 the Mn seem to take the place of Mg in the iron phase. This can be seen from the EDS analysis, where

for L1 the Mg amount was at 12.5 in the AlSiFeMg phase. In L5 the Mg amount is only at 0.3-0.4, while the Mn amount has jumped to around 10 in what is now a AlSiFeMn phase. This proves that when adding more Manganese and Iron into a Al-Si-Mg alloy, the Al-Si-Mg-Fe phase will eventually be replaced by the Al-Si-Mn-Fe phase. The Magnesium will segregates into the alloy.

It is reasonable to believe that the Mg_2Si precipitate phase is found in the Al-SiFeMg phase from the EDS analysis, but the phase is not big enough to spot. This phase seem to be even smaller for L5 where the magnesium has segregated.

Other observations form the mapping is that the addition of the other elements like Zn, Ni and Cu can be detected in the L5 but in very vague detection. It seems that the Zn is dissolves into the material. The nickel and copper is very hard to detect, but the Ni if present seem to dissolve into the material as well. While the Cu follows the iron phase.

The mapping showed that the modification of the silicon eutectic had worked, with fine particles, both for L1 and L5. Proving that the modification hasn't been effected by the addition of the alloying elements.

5.6 Electrical conductivity

The results from the sigma test showed that the electrical conductivity does not variate much from between the alloys. Variating from an average value at 21.34 MS/m at the lowest to 22.24 MS/m, is not a great difference. This means that the addition of more recycled aluminium does not change the electrical conductivity significantly. However the trend seem to be that the small decreases detected comes when adding more alloying elements, so a further increase in this may lower the electrical conductivity even further.

5.7 Summary

Both from the tensile tests and the pictures from the optical microscope can it be stated that the strontium modification has worked well. If it hadn't work as it should then it would have much less plastic deformation, close to nothing. Causing the material to be less ductile. The grain size does also seem to follow the same trend as the mechanical properties, where the larger average grain size has the highest properties. This is opposite to what is common where a finer grain structure will give better mechanical properties, so this is most likely a coincidence.

The addition of Mn and Fe seem to effect the formation of Mg_2Si precipitates, in an negative way. This may cause the tensile properties to worsen, since the formation of Mg_2Si during ageing is a big contributor to these properties. This could be the explanation to why the tensile properties drops from L3 to L5.

Chapter 6

Conclusion

The addition of alloying elements to a aluminium alloy does have an effect on the mechanical properties. In this study it was that the addition of increasing amount of Zn, Mn, Cu, Ni and Fe to an AlSiMg alloy effects the mechanical properties like yield strength, UTS, ductility and fracture toughness. It was found that the L3 alloy, the one with the middle amount of alloying elements had the best properties. The elastic zone of the alloys where all consistent while the plastic zones had large variations due to the porosity.

An optimal heat-treatment program for the alloys where investigated and found that the T6 heat-treatment program suited best. With solution heat-treatment at 535°C for 8h, water quenching and artificial aging at 175°C for 8h. This heat-treatment gave an increase in yield strength from 111 MPa to 270 MPa for L3. Proving that the heat-treatment had worked as desired.

It was also found that the hardness of each of the alloys was not significantly effected by the addition of a various amount of alloying elements. The same can be said for the electrical conductivity.

The results from the SEM showed that the addition of more Mn and Fe to an AlSiMg alloy causes the phases containing magnesium to be "replaced" by the manganese. In the phases containing magnesium small Mg_2Si precipitates thought to be found here as an effect of the heat-treatment. The addition of Mn and Fe, causes this phase to segregate.

From the results gathered throughout this project, it is reasonable to conclude that the use of recycled aluminium in the casting process is a good idea as long as it is not added in to large amounts. With the environmental and economical advantages gained from use of recycled aluminium, the use of recycled aluminium would be recommended for this casting process.

6.1 Further Work

Since this master thesis was interrupted and shortened down due to COVID-19. Some experimental aspects that was planned but not conducted is still relevant to complete. The main experiment to be conducted is a corrosion test. It would be very relevant to test how the various alloys is effected by corrosion, since the casted products is supposed to be used in an maritime environment where corrosion is an important problem.

Since some of the alloys had a different composition than what was meant, a new casting of these alloys and completion of the same test would be advised. Investigating the effect of each of the alloying elements was also planned as part of this project, so casting new samples while adding only one alloying element to each alloy. This would help give an understanding as to what the different alloying elements does to the aluminium alloy.

References

[1] D. Callister and D. Rethwisch. *Materials Science and Engineering*. John Wiley & Sons (Asia) Pte Ltd, 2011.

[2] T. Ebbesen. *Aluminium in Marine Components and the Use of Secondary Aluminium*. Department of Material science and Engineering, 2019.

[3] G. Sigworth. *ASM Handbook: Aluminium Casting Alloys and Casting Processes*. Vol. 2A. ASM International, 2018.

[4] O. Fayoumi and U. N. "Effect of Alloying Element on the Integrity and Functionality of Aluminium-Based Alloy." In: (2017).

[5] D. Kopeliovich. "Effects of Alloying Elements on Properties of Aluminium Alloys." In: (2012). URL: https://www.substech.com/dokuwiki/doku.php?id=effects_of_alloying_elements_on_properties_of_aluminum_alloys.

[6] VDS. *Influence of Copper on the Corrosion Resistance of Al-12%Si Casting Alloy*. Vol. 77. Metallurgia, 1968.

[7] R. Rana and D. S. *Reviews on the Influences of Alloying elements on the Microstructure and Mechanical properties of Aluminium Alloys and Aluminium Alloy Composites*. International Journal of scientific and Research Publications, 2012.

[8] AloTec. "How and why alloying elements are added to aluminium." In: (2015). URL: http://www.alcotec.com/us/en/education/knowledge/qa/How-and-why-alloying-elements-are-added-to-aluminum.cfm.

[9] D. Yang H. Watson and Y. Wang. "Effect of nickel on the microstructure and mechanical property of die-cast Al–Mg–Si–Mn alloy." In: (2014).

[10] M. Wang X. Guo and L. Zhuang. *Effect of Zn on microstructure, texture and mechanical properties of Al-Mg-Si-Cu alloys with a medium number of Fe-rich phase particles, Materials Characterization*. Vol. 134. 2017.

[11] M. Remøe. *The Effect of Alloying Elements on the Ductility of Al-Mg-Si Alloys*. Institutt for materialteknologi, 2014.

[12] M. Schlesinger. *ASM Handbook: Recycling of Aluminum*. Vol. 2A. ASM International, 2018.

[13] M. Tangstad. *Metal production in Norway*. Akademika Publishing, 2013.

[14] R. Sisson. *Encyclopedia of Materials: Science and Technology (Second Edition)*. Elsevier, 2001.

[15] G. Sigworth. *ASM Handbook: Heat Treatment of Aluminium Alloy Castings*. Vol. 2A. ASM International, 2018.

[16] J. Weritz. *The Aluminum Association Alloy and Temper System*. The Aluminum Association, 2016.

[17] G. Totten and D. MacKenzie. *ASM Handbook: Principles of Heat Treating of Nonferrous Alloys*. Vol. 4E. ASM International, 2016.

[18] D. MacKenzie and N. Bough. *ASM Handbook: Quenching of Aluminium Alloys*. Vol. 4E. ASM International, 2016.

[19] G. Sigworth. *ASM Handbook; Aluminum Casting Alloys and Casting Processes*. Vol. 2A. ASM International, 2018.

[20] W. Kurz and J. Fisher D. *Fundamentals of Solidification*. Trans tech publications LTD, 1998.

[21] R. Lumley. *Fundamentals of Alumnium Metallurgy: Production, Processing and Applications*. Elsivier Science and Technology, 2010.

[22] D. Stafanescu and R. Ruxanda. *ASM Handbook: Solidification Structures of Aluminum Alloys*. Vol. 9. ASM International, 2018.

[23] G. Sigworth. *ASM Handbook; Modification of Aluminium-Silicon Alloys*. Vol. 15. ASM International, 2008.

[24] D. Breakey. "Stress-Strain Curve." In: (2008). URL: `https://en.wikipedia.org/wiki/File:Stress_Strain_Ductile_Material.pdf`.

[25] ASTM. *ASTM Standard E112; Standard Test Methods for Determining Average Grain Size*. 2013.

[26] G. Revenkar. *ASM Handbook: Introduction to Hardness Testing*. Vol. 8. ASM International, 2000.

[27] G. Vander Voort. *ASM Handbook: Microindentation Hardness Testing*. Vol. 8. ASM International, 2000.

Appendix A

Measurements

A.1 Measurements

A.1.1 Heat-treatment

Table A.1: Table of results from hardness test on L1 sample 1 at 160°C.

	2h [HV1]	4h [HV1]	8h [HV1]	16h [HV1]
1	88.6	100.1	107.1	110.6
2	98.4	112.9	103.1	116.8
3	89.94	98.09	100.8	119.9
4	75.21	118.9	109.3	104.3
5	82.62	115	105.7	112.2
6	92.67	112.2	121.1	108.2
7	98.76	96.95	106.3	114.7
8	96.35	95.41	114	135.8
9	92.82	92.47	124.7	117.5
10	92.15	94.07	108.4	115.9
Average	90.752	103.609	110.05	115.59

Table A.2: Table of results from hardness test on L1 sample 2 at 160°C.

	2h [HV1]	4h [HV1]	8h [HV1]	16h [HV1]
1	95.92	112.8	112.1	105.3
2	91.71	110.9	102	113.1
3	87.02	96.78	107.7	99.16
4	90.09	101.5	114.3	93.99
5	95.07	107.2	109	116.7
6	90.8	105.6	101.6	111.8
7	87.25	101.9	103.5	100.1
8	87.02	92.07	77.37	112.8
9	76.38	113.9	104.8	114.3
10	95.07	107.6	115.4	115.2
Average	89.633	105.025	104.777	108.245

Table A.3: Table of results from hardness test on sample 1 at 175°C.

	2h [HV1]	4h [HV1]	8h [HV1]	16h [HV1]
1	107.4	113.6	95.28	119.8
2	108.3	110.3	99.57	105
3	116.4	116.3	113.9	118.8
4	116.8	102.2	114.5	105
5	113.9	111.8	113.1	109.4
6	109	113.8	112.3	120.9
7	103.6	109.6	114.7	124.6
8	104.1	109.2	117.3	109.3
9	115.3	127.1	100.8	111.1
10	109.1	111	112.3	117.4
Average	110.39	112.49	109.375	114.13

A.1.2 Tensile test

Table A.4: Table of results from hardness test on sample 2 at 175°C.

	2h [HV1]	4h [HV1]	8h [HV1]	16h [HV1]
1	107	110	115.9	110.7
2	110.5	111.2	112.5	109.1
3	111.8	113	104	116.9
4	110.8	111.8	114.8	106.2
5	109.8	111.4	120.8	103.7
6	110.5	113.4	117.2	110.4
7	114	95.92	117.9	114.1
8	108.6	110.7	105.4	113.4
9	106.9	101.7	126.4	110.5
10	109.1	110	122.5	107.4
Average	109.9	108.912	115.74	110.24

Table A.5: Table of results from hardness test on sample 1 at 190°C.

	2h [HV1]	4h [HV1]	8h [HV1]	16h [HV1]
1	103.6	116.6	100.9	105.1
2	103.9	115.1	95.32	96.43
3	104.4	111.6	113.3	104
4	103.4	112.2	98.53	100.5
5	103.9	104.8	104.3	113.4
6	91.15	106.4	91.83	98.27
7	104.7	108.9	96.26	105.4
8	94.78	100.9	98.89	98.67
9	79.5	110.9	90.05	102.8
10	104.2	103.8	101.2	98
Average	99.35	109.12	99.06	101.69

Table A.6: Table of results from hardness test on sample 2 at 190°C.

	2h [HV1]	4h [HV1]	8h [HV1]
1	108.9	108.5	109.6
2	118.6	120.4	102.7
3	112.4	34.3	99.61
4	113	111.9	107.6
5	104.3	118	113.6
6	112.9	112.4	95.92
7	111.6	104.3	102.4
8	110	107.4	110.4
9	114.4	104.3	92.59
10	106.8	99.84	109.4
Average	111.29	102.134	104.382

Table A.7: Table of calculated values after tensile testing for L1.

	1	2	3	4	Average
Strain at break [%]	0.94	1.74	0.85	1.16	1.17
E-Modulus [GPa]	61.7	62.1	59.2	63.2	61.55
Tensile stress at maximum load [MPa]	233.2	254.6	235.1	256	244.73
Tensile stress at yield [MPa]	224.2	229.1	225.4	237.8	229.13

Table A.8: Table of calculated values after tensile testing for L2.

	1	2	3	4	Average
Strain at break [%]	0.83	1.21	1.12	0.69	0.96
E-Modulus [GPa]	64	65.9	64	60.2	63.53
Tensile stress at maximum load [MPa]	253.1	276.3	269.5	239.4	259.58
Tensile stress at yield [MPa]	244.5	259.2	248.3	232.3	246.08

Table A.9: Table of calculated values after tensile testing for L3.

	1	2	3	4	Average
Strain at break [%]	1.49	0.97	0.63	1.04	1.033
E-Modulus [GPa]	64.4	67.1	61.8	66	64.83
Tensile stress at maximum load [MPa]	283.3	268.2	254.8	274.6	270.23
Tensile stress at yield [MPa]	262.8	258.9	253.7	262.8	259.55

Table A.10: Table of calculated values after tensile testing for L4.

	1	2	3	4	Average
Strain at break [%]	0.94	0.9	0.67	1.09	0.9
E-Modulus [GPa]	63	61	62.6	62.9	62.38
Tensile stress at maximum load [MPa]	267.4	253.5	251.2	269.6	260.43
Tensile stress at yield [MPa]	256.3	245	251	252.3	251.15

Table A.11: Table of calculated values after tensile testing for L5.

	1	2	3	4	Average
Strain at break [%]	0.68	1.06	0.61	0.81	0.79
E-Modulus [GPa]	61.5	66.6	66.1	66.4	65.15
Tensile stress at maximum load [MPa]	237.7	276.4	244	267.3	256.35
Tensile stress at yield [MPa]	234.3	238.6	261.4	253.4	246.93

A.2 Pictures

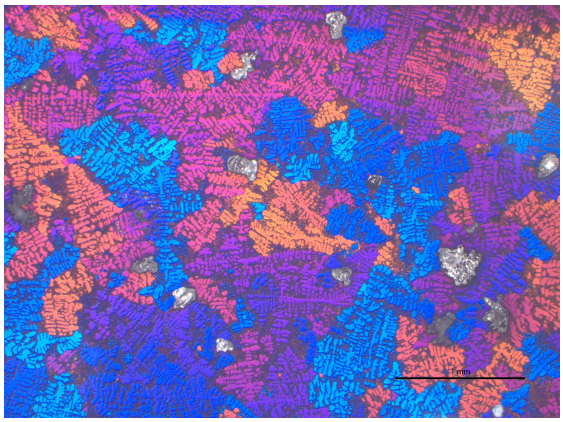

(a) OM picture of L1 2.5x magnification.

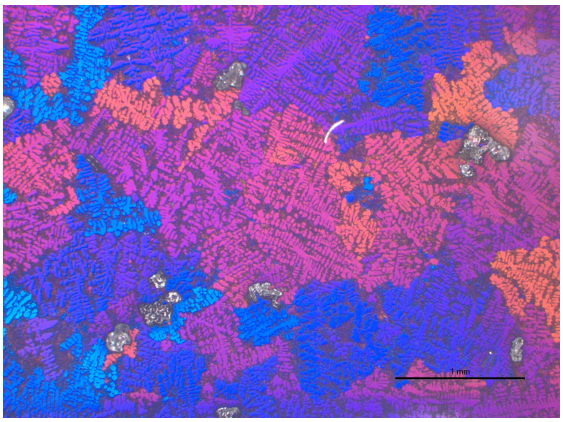

(b) OM picture of L1 2.5x magnification.

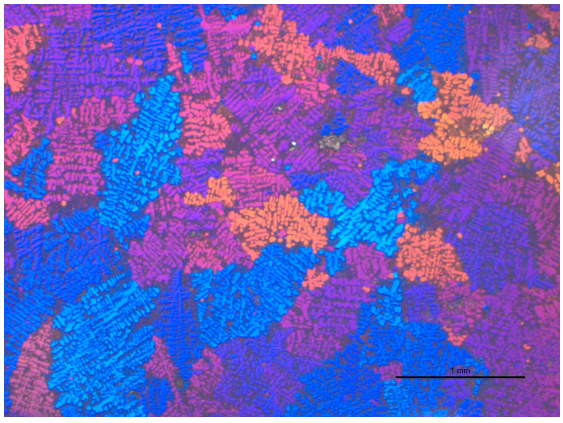

(a) OM picture of L2 2.5x magnification.

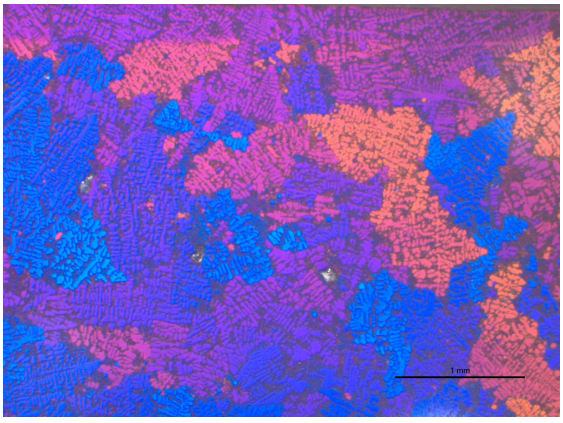

(b) OM picture of L2 2.5x magnification.

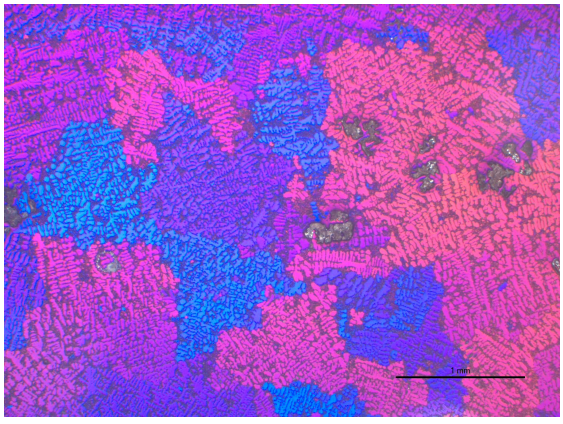

(a) OM picture of L3 2.5x magnification.

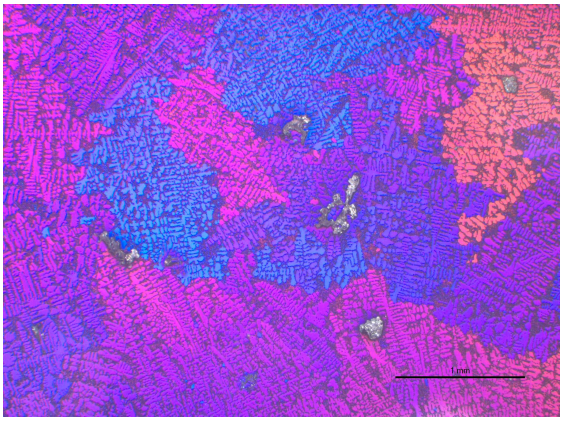

(b) OM picture of L3 2.5x magnification.

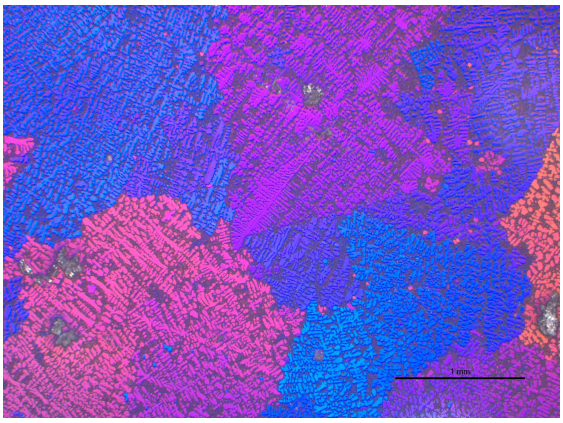

(a) OM picture of L4 2.5x magnification.

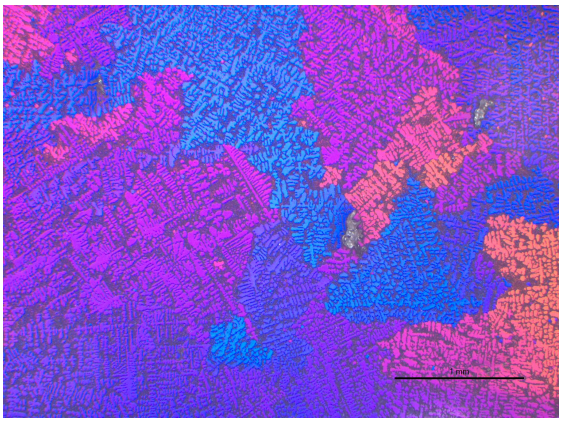

(b) OM picture of L4 2.5x magnification.

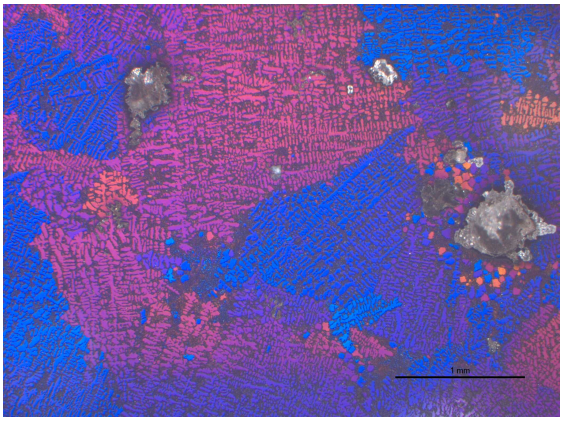

(a) OM picture of L5 2.5x magnification.

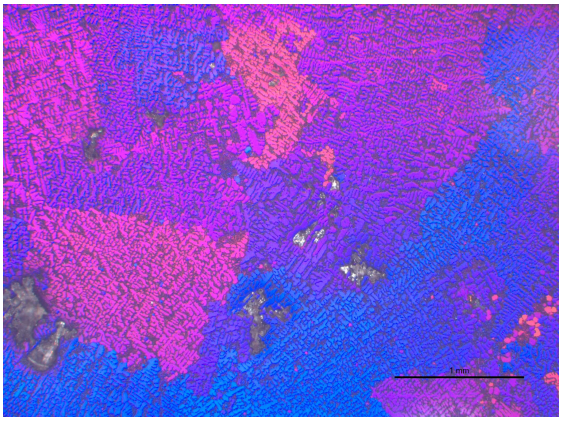

(b) OM picture of L5 2.5x magnification.

NTNU

Norwegian University of
Science and Technology